2016

Climatic Cycles Recorded in Glacially Influenced Rhythmites of the Gowganda Formation, Huronian Supergroup

Tim S. Howe
The University of Western Ontario, thowe3@uwo.ca

Patricia L. Corcoran
The University of Western Ontario, pcorcor@uwo.ca

Fred Longstaffe
The University of Western Ontario, flongsta@uwo.ca

Elizabeth A. Webb
The University of Western Ontario, ewebb5@uwo.ca

R Gerhard Pratt
The University of Western Ontario, gpratt2@uwo.ca

Climatic cycles recorded in glacially influenced rhythmites of the Gowganda Formation, Huronian Supergroup

T. S. Howe*, P. L. Corcoran, F. J. Longstaffe, E. A. Webb, R. G. Pratt

Department of Earth Sciences, The University of Western Ontario, London, Ontario, N6A 5B7, Canada

*Corresponding author (e-mail: thowe3@uwo.ca)

Abstract: The Gowganda Formation of the 2.45-2.2 Ga Huronian Supergroup contains glacially-induced, varve-like rhythmites that potentially preserve a detailed record of climatic conditions during the Paleoproterozoic Era. Four rhythmic couplet thickness records were measured at two outcrops near Wharncliffe, Ontario for the purpose of time-series analysis. The couplets, which range from 1 – 32 mm thick, are composed of alternating layers of siltstone and claystone. Time-series analysis of the couplet thickness records using the MTM Toolkit of Mann and Lees (1996) consistently revealed periodicities in the range of 2.2-2.9 couplets per cycle, which is consistent with climatic cycles such as the quasi-biennial oscillation (QBO) and the El Niño Southern Oscillation (ENSO) observed in modern times. This periodicity suggests that the rhythmic couplets represent annual deposits (i.e. varves). Evidence for the presence of cycles at 3.0-4.9 couplets, 6.6-6.9 couplets, 8.8-9.2 couplets, 22.8 couplets, and 30.1-31.0 couplets were also observed in some couplet thickness records; however the presence of these longer term cycles was inconsistent from site to site.

Keywords: Huronian Supergroup, Gowganda Formation, varves, rhythmites, Paleoproterozoic, MTM Toolkit, time-series analysis

1. Introduction

Clastic rhythmites are subaqueous sediment couplets that are deposited in horizontal layers on a periodic basis (Bramlette, 1946; Reineck and Singh, 1972). The couplets composing a rhythmite generally consist of a coarse-grained layer, predominantly composed of fine sand or coarse silt, and a fine-grained layer, which is generally composed of fine silt or clay (Williams, 2000). Rhythmite development may be predominantly influenced by depositional environments and processes, which is the case for tidalites and turbidite deposits, or mainly by climatic conditions at the time of deposition, particularly if they are formed in association with deglaciation. De Geer (1912) was the first researcher to describe rhythmites that form annually as a result of deglaciation, introducing the term “varve” to describe a couplet. Early work on varves found in glacial lakes in eastern Canada noted that the summer, coarse-grained layers were substantially thicker than the winter, fine-grained deposits (Antevs, 1925). However, each layer comprising a varve is not necessarily homogenous, as shown in a later investigation of varves in Lake Barlow-Ojibway, Ontario, Canada (Agterberg and Banerjee, 1969). The authors subdivided the winter layer into a lower turbidite deposit overlain by a clay layer that rained out from suspension. More recently, varves have been defined as containing two or more laminal layers that repeat annually (Ojala et al., 2012). Ultimately, the thickness of individual varves in glacially-influenced environments is related to the annual influx of sediment to a regional basin, which is influenced by the annual rate of glacial meltwater discharge (Delaney, 2005).

Hughes et al. (2003) conducted a small-scale spectral analysis of 256 rhythmites within the upper Gowganda Formation from a location they referred to as the Wharncliffe argillite. The present study expands upon the work of Hughes et al. (2003) by examining four rhythmite sequences from two rock outcrops within the upper Gowganda Formation in order to: (1) determine whether climate forcing can be identified, and if found, (2) compare climatic periods across all four rhythmite records. We employ high resolution spectral analysis using the multitaper method of Mann and Lees (1996) to identify consistent periodicities associated with climatic forcing influenced rhythmite formation, implying that individual rhythmites may represent annual deposits.

2. Geologic Setting

The Huronian Supergroup is a sedimentary-dominated succession that unconformably overlies Archean rocks of the Superior Province north of Lake Huron in Ontario, Canada (Fig. 1). The succession forms an approximately 325 km long belt that extends from Noranda, Quebec in the northeast to the Sault Ste. Marie area in the west (Willingham et al., 1985). The Huronian Supergroup is up to 12 km thick at its southern boundary where it underlies Paleozoic rocks of the Michigan Basin (Young et al., 2001), and thins toward the north and west of the Southern Province. The southeastern boundary of the Huronian Supergroup is characterized by the Grenville Front, the remnants of a mountain building event that terminated at ca. 1.0 Ga (Moore and Thompson, 1980). Rocks in the Bruce Mines-Elliot Lake area have been metamorphosed to greenschist grade (Lindsey, 1969), but the prefix “meta” to describe the rock types is herein omitted for simplicity. Tectonic deformation in the area between Sault Ste. Marie and Elliot Lake ranges from low to moderate, and is characterized by upright, open folds with gently plunging hinges (Bennett, 2006). Tectonic structures are poorly developed, and the beds in the study area dip between 4 and 30 degrees. It is therefore unlikely that rhythmite thicknesses have been greatly modified.

The maximum age of the Huronian Supergroup is 2450 +25/-10 Ma, based on U-Pb zircon analysis of the Copper Cliff Formation (Fig. 2; Krogh et al., 1984). The minimum age of the Huronian Supergroup was determined to be 2217.0±6.0 Ma based on U-Pb analysis of primary baddeleyite from the Nipissing gabbro dikes that intrude the succession (Corfu and Andrews, 1986). Tang and Chen (2013) suggested that the duration of the Huronian glaciation events could be constrained to 2.29-2.25 Ga, given their similarity to diamictite deposits in the Turee Creek Group, Hammersley Basin, Western Australia; Makganyene Formation, Griqualand West Basin, South Africa; Boshoek Formation and Duitschland Formation, Transvaal Basin, South Africa; Sariolian Group, Karelian Supergroup, Eastern Baltic Shield, Russia; Chocolay Group, Marquette Range Supergroup, Michigan/Wisconsin USA; and Snowy Pass Supergroup, Wyoming, USA. Rasmussen et al. (2013) report a ca. 2.31 Ga U-Pb age from a purported tuff in the Gordon Lake Formation, upper Huronian Supergroup, suggesting that most of the Huronian formations are older than 2.31 Ga. The lower Huronian units (pre-Gowganda Formation) are interpreted to have been deposited in transtensional to extensional (synrift) basins whereas the upper Huronian Supergroup represents passive margin deposits (Young and Nesbitt, 1985; Mustard and Donaldson, 1987; Holm et al., 2005; Eyles, 2008; Young, 2013).

The Hough Lake, Quirke Lake and Cobalt groups represent tripartite cycles, with each containing glacial diamictite (poorly sorted, matrix-supported conglomerate) at their bases, followed up-section by thinly laminated siltstone and claystone that are, in turn, overlain by arenaceous sandstone (Young et al., 2001). This complex period of glaciation has been identified in the literature as the ‘Huronian Glacial Event’. Striations and grooves on rock surfaces underlying the diamictite, striated and faceted clasts within the diamictite, and the presence of lonestones/dropstones in the fine-grained laminated deposits all support a glacial interpretation for the basal units of the middle three Huronian groups (Lindsey, 1969; Young, 1970). The argillites (meta-mudstones) and claystone/siltstone rhythmites that dominate the middle sections of each formation have been interpreted as post-glacial deltaic deposits (Lindsey, 1969; Young et al., 2001). The third stage of each glacial cycle is represented by cross-bedded, medium- to coarse-grained sandstones interpreted as having been deposited in shallow marine, fluvial-deltaic or fluvial environments (Palonen, 1973; Long, 1978; Young et al., 2001).

Interbedded siltstones and claystones that characterize the upper part of the Gowganda Formation are inferred to represent a prodeltaic succession that was deposited as a continental ice sheet retreated (Rainbird, 1985; Young et al., 2001; Long, 2009). The present study focuses on the rhythmic deposits of the Gowganda Formation in the Bruce Mines/Elliot Lake area. One of the outcrops, referred to as Outcrop A (the Wharncliffe argillite of Hughes et al., 2003), is located adjacent to Highway 129, approximately 25 km north of Thessalon and 4 km north of Wharncliffe, Ontario (Fig. 3). A second outcrop, Outcrop B, is located approximately 4 km east of Outcrop A on County Road 554. A sedimentological analysis of the lithofacies in the study area was conducted by Howe (2015) and is presented in Table 1.

3. Evaluating Rhythmic Deposits using Cyclostratigraphy

Cyclic stratigraphic processes such as sedimentation can be described and interpreted as periodic oscillations. A periodic oscillation is mathematically described using a simple sinusoidal curve consisting of a fixed amplitude, frequency and phase. Geological oscillations describing cyclic stratigraphy are more complex in shape, and can be represented as a sum of multiple oscillations with particular frequencies. Multiple frequencies comprise a spectrum, and the analysis of a spectrum is called spectral analysis (Weedon, 2003). Where stratigraphic thicknesses are sequentially measured at constant intervals, based on observable parameters such as recognizable couplets, a cyclostratigraphic series of thickness vs cycle number analogous to a time series can be formed, if three conditions are met: (1) environmental conditions are presumed consistent throughout deposition of the facies, (2) the thickness of any individual bed results from the influence of a single environmental variable, and (3) there is a relationship between the thickness of any individual bed, and time (Weedon, 2003). In tidal or glacial depositional environments where discrete sedimentation occurs, variations in bed thickness represent a modification of the environment over time. The cyclostratigraphic series can be used to calculate cyclostratigraphic spectra using well known methods of time series analysis. Care must be taken not to identify the original data series with specific units of time, and the horizontal axes are always referred to herein as “couplets”. Similarly the resulting spectra will quantify the distribution of underlying periodicities in terms of couplets per cycle. For the purpose of spectral analysis, it is assumed that the stratigraphic record is composed of regular components (the signal) and irregular components (the noise). The signal represents a periodic oscillation in some variable whereas the noise represents an irregular oscillation (Weedon, 2003).

Many studies have used spectral analysis to evaluate rhythmic deposits for periodicities that may reflect the process of deposition (e.g. Williams 1985; Williams 1989; Godsey et al. 1999; Rittenour et al., 2000; Hughes et al., 2003; Breckenridge, 2007; Andrews et al. 2010). Rhythmite sequences in the Gowganda Formation have previously been considered as potential glacial varves (Lindsey, 1969; Hughes et al., 2003), and therefore may represent some of the oldest deglaciation deposits on Earth. However, tidal rhythmites (Williams, 1981; Williams, 1985; Williams 1989) and turbidites (de Alvarenga and Trompette, 1992; Martins-Neto et al. 2001) in the Proterozoic rock record can also present facies that are strikingly similar to varves. Thus, one of the challenges facing the study of Paleoproterozoic rhythmites is that annual control may be inferred, but not conclusively established, due to a lack of biogenic markers in the Precambrian rock record.

4. Methods

The rhythmite units in Outcrop A and Outcrop B (Fig. 4) are morphologically similar, and are up to 15 and 7 m thick, respectively. Selected rhythmite sections were measured at each outcrop with a tape measure for the purpose of spectral analysis. Outcrop A and Outcrop B emerge from the local soil on an angle, increasing in exposure height from north to south, and thus they were measured in a stair-case fashion, with the bottom of each section being horizontally continuous with the top of the previous section. Each couplet was measured from the base of a siltstone bed, which generally had higher relief, to the top of the overlying claystone bed.

The rhythmites at Outcrop A were separated into a lower and upper record by a 109 cm thick bed that resembles a slump deposit. Therefore, the two records comprise sequential, but discontinuous data sets. The lower record had a total thickness of 180 cm, and was composed of couplets ranged from 1 - 18 mm thick, with an average thickness of about 7±3 mm (reported as standard deviation (SD) here and elsewhere; Fig. 5). The rhythmite measurements in the lower record of Outcrop A do not display a trend of either increasing or decreasing thickness. The upper record of Outcrop A contained a total thickness of 5 m. The average couplet thickness for the upper record of Outcrop A was ~9±5 mm, with couplet thickness measuring 1 - 32 mm (Fig. 5). The data from the upper record of Outcrop A shows a general increase in rhythmite thickness up-section, which indicates an increasing sedimentation rate that may have been a result of increased glacial melting under a warming environment (Ridge et al., 2012).

Two records were also measured at Outcrop B. The lower and upper records of Outcrop B are separated by 80 cm of rhythmites that were too fractured to measure, and thus both records of Outcrop B comprise sequential, yet discontinuous data sets. The lower record contained a total thickness of 300 cm. The couplets ranged in thickness from 3 - 31 mm, with an average of ~13±5 mm (Fig. 6). The upper record of Outcrop B measured a total thickness of 150 cm, with couplets ranging in thickness from 5 - 28 mm (average = ~12±4 mm; Fig.6). The thickness measurements from both the lower and upper records of Outcrop B do not indicate an overall trend of increasing or decreasing thickness, which may indicate a period of steady sedimentation or reflect data sets that are too small to indicate an overall trend. Although the rhythmites of

Outcrop A and Outcrop B are morphologically similar, it is not known whether they represent the same, different, or overlapping depositional events.

Periodic cycles are often not visually apparent in raw data sets, and thus a spectral analysis of a raw data set can be employed to identify periodicities. Spectral analysis of the rhythmite measurements was conducted using the multitaper method ("MTM") as included in the MTM Toolkit of Mann and Lees (1996). The MTM is a non-parametric method that employs the discrete Fourier transform, and uses the average of multiple independent trials to estimate power spectra (Thomson, 1982). In a climate time series, the MTM can be used to separate climatic signals from the background noise in which they exist (Mann and Lees, 1996). Mann and Lees (1996) describe the background noise in climate systems as "red noise", which is defined to be composed of white noise and an enhanced, low-frequency, slow-response climate signal such as that induced by the thermal inertia of the oceans. Red noise may comprise a significant proportion of the time series, leading to a low signal-to-noise ratio. The MTM Toolkit of Mann and Lees (1996) uses a first-order autoregressive (AR(1)) process to model the noise level, and fits this model to the data in order to estimate the noise. The AR(1) process expresses each sample in a time series as a linear combination of the previous sample and a white noise contribution. By applying the AR(1) process to white noise, the lower frequencies are naturally enhanced, leading to a red noise spectrum. The MTM combined with the red noise model allows for improved noise identification, which leads to enhanced statistical significance of identified signals. In this study, the datasets are sufficiently small to allow for the use of 3 tapers (where the number of tapers used is K = 2p -1) and a time-frequency bandwidth p of 2; these parameters were used throughout the study.

5. Results

Couplet measurement data provided by Gary Hughes (used in the Hughes et al. 2003 study) were processed using the MTM Toolkit (Fig. 7). Spectral analysis results from the measurements at Outcrops A and B are provided in Figures 8 and 9. In these figures, ”harmonic peaks” represent periodic signals that correspond to singular peaks in the power spectrum estimated by the MTM; the “reshaped” spectrum is calculated using a modified version of the reshaping process of Thomson (1982),the AR(1) red noise spectrum is estimated from the median-smoothed spectrum to provide a robust model for the noise background, and the “median” line depicts the red-noise fit to the median-smoothed spectrum (calculated by replacing each frequency point in the reshaped spectrum with its median value). Three confidence levels are used to evaluate the distribution of the frequency as depicted by the reshaped spectrum, relative to background noise: 90%, 95% and 99% (Figs. 7-9).

The MTM results produced from the Hughes et al. (2003) data (Fig. 7) are similar to the published results in that paper. In the MTM results from the lower record of Outcrop A (Fig. 8) quasi-periodic cycles of 4.4 and 9.2 couplets were detected with a 90% degree of certainty. Quasi-periodic cycles of 2.2 and 6.6 couplets were detected with a 95% degree of certainty, and a quasi-periodic cycle of 2.9 couplets was detected with a 99% degree of certainty. In the MTM results from the upper record of Outcrop A (Fig. 8), a number of quasi-periodic cycles in the range of 2.3 to 4.4 couplets were found, in addition to quasi-periodic cycles of 4.9 and 8.8 couplets, all having a 90% degree of certainty. A quasi-periodic cycle of 22.8 couplets, having a 95% degree of certainty, was also identified. Quasi-periodic cycles of 56.9 and 31.0 couplets (99% certainty) were also evident, in addition to a harmonic cycle of 2.4 couplets.

The MTM results from the lower record of Outcrop B (Fig. 9) show a number of quasi-periodic cycles in the range of 2.3 to 4.4 couplets, and a quasi-periodic cycle of 30.1 couplets, all with a 90% degree of certainty. A harmonic cycle of 2.8 couplets was also observed. The results from the upper record of Outcrop B (Fig.9) indicate a quasi-periodic cycle of 6.9 couplets having a 99% degree of certainty, and minor quasi-periodic cycles in the range of 2.9 to 3.4 couplets (90% - 95% degree of certainty).

6. Discussion

6.1. Comparisons with tidal rhythmites

Varves are difficult to conclusively identify in the Precambrian rock record because of the lack of time indicators, such as summer deposition of pollen, that allow for interpretations of annual control. The potential result is misinterpretation of tidal-induced rhythmites as varves. Rhythmically laminated sediments deposited from tidal activity are called tidal rhythmites or tidalites (Klein, 1971; Chan et al., 1994). Tidal rhythmites are composed of alternating sandstone/siltstone and claystone laminations that reflect the flood and ebb stages of diurnal or semidiurnal tides. Traction currents operating during the flood and ebb stages of a tidal cycle deposit coarse-grained (silty) sediment, whereas fine-grained (muddy) material is deposited during the slackwater period when the flow direction alternates (Klein, 1971). Although tidal rhythmites may resemble varves in the rock record, changes in the lunar and solar cycles influence the strength of tidal flow, resulting in periodic variations in bed thickness (Williams, 1989). Maximum rhythmite thickness occurs at the peak of the spring tide, with rhythmite thickness decreasing as the tide cycle progresses to the neap tide (Archer et al., 1990). Typically, the planar-laminated silty layers are much thicker than the thin clay drapes that overlie them (Archer et al., 1995). In Precambrian tidal settings, the lunar month has been estimated to contain between 30.5 days (Williams 1989; Williams 1991) and 32 days (Mazumder, 2004).

Precambrian varves can be distinguished from tidalites based on morphology (e.g. Hughes et al. 2003; Andrews et al. 2010), sedimentology, and/or spectral analysis results that preclude tidalite-like periodicities. In this study, the rhythmites typically have claystone layers that are thicker than the siltstone layers (Table 1), and the opposite would be expected if the rhythmites were tidalites. In addition, a pronounced cycle of rhythmite thickening and thinning typical of tidalites (Archer et al., 1990), was not observed (Fig. 4). The rocks studied contain no sedimentary structures consistent with a tidally-influenced setting, such as mud cracks, reactivation surfaces, or herringbone cross stratification. Morphological, sedimentological and spectral analysis observations, therefore, strongly suggest that the rhythmites are not tidalites. In addition, the sedimentation rate in this study ranges from 1-32 mm per rhythmic cycle, which compares favorably with typical Holocene varves that measure from 1 mm to more than 50 mm thick (Godsey, 1999; Rittenour, 2000; Breckenridge, 2007). Given the available evidence, combined with the presence of dropstones in some of the rhythmite layers, we hypothesize that the rhythmites could represent annual depositional cycles. In the following section we examine the implications of such a hypothesis, and we present evidence that the resulting periodicities are consistent with periodicities seen in modern climate systems.

6.2. Consistent Periodicities

If the deposits of Outcrop A are considered to represent annual rhythmites and a similar interpretation is extended to Outcrop B, then the results of this study can be compared to those of Hughes et al. (2003) (Table 2), and to those determined from investigations of Holocene and Pleistocene varves. With one exception, the MTM Toolkit identified peaks in the Hughes data similar to those published in Hughes et al. (2003), thereby validating the method used. A cluster of periodicities within the range of 2.2 – 2.9 couplets per cycle was determined from all four of the rhythmite records in this study, as well as from the data of Hughes et al. (2003), and from studies of varves in Lake Superior (Breckenridge, 2007), glacial Lake Hitchcock (Rittenour et al., 2000) and Lake Huron (Godsey et al., 1999) (Table 3). If the couplets do correspond to annual deposition beds, then cycles within this range (2.2 – 2.9 years per cycle) are reminiscent of the modern day quasi-biennial oscillation (QBO), which is a periodic change in stratospheric equatorial wind directions that cyclically varies with a period of 22 to 34 months (Baldwin et al., 2001). The QBO impacts the stratospheric polar vortex, which in turn influences weather patterns on the surface of the Earth. Godsey et al. (1999) also attributed periodicities within the range of 2 - 3 years to the Southern Oscillation Index, which is a measure of air pressure fluctuations resulting from ocean temperature differences between the western and eastern tropical Pacific.

A number of low periodicity events within the range of 3.0 – 6.9 couplets per cycle were also determined from the four rhythmite records in this study. Godsey et al. (1999) and Rittenour et al. (2000) attribute periodicities of three to seven years to climatic fluctuations associated with ENSO, the El Niño – Southern Oscillation. Hughes et al. (2003) and Breckenridge (2007) attribute periodicities of three to six years to ENSO, and periodicities of six to seven years to NAO, the North Atlantic Oscillation. If the hypothesis of annual deposition is accepted, then it is apparent that these periodicities are also present in the Gowganda Formation. The sediment record therefore hints that climate systems similar to QBO and ENSO may have been operational during the Paleoproterozoic, and supports the hypothesis that these ancient rhythmic couplets were deposited on an annual basis.

6.2. Inconsistent Periodicities

Table 2 indicates that some periodicities do not appear in all records, indicating that they may not preserve climatic cycles, and they are thus, not considered here. There are a number of reasons why certain periodicities may be observed in only one or two records. These inconsistencies may arise from variations in depositional environments. The couplets at Outcrop A are composed of claystone and siltstone, whereas the couplets at Outcrop B are composed of fine- and coarse-grained siltstone. This variance may be attributed to different locations within one deltaic environment, different locations in separate deltaic or basinal environments, temporal variations in deposition, or a combination of these factors. In addition, if glacial melting ceases completely for an extended time period, there is no accounting for the “missing data” in the spectral analysis model.

The depositional environment for the upper Gowganda Formation in the study area is dynamically complex, with sedimentation that may have been influenced by both delta progradation and glacial recession (Howe, 2015). Locally, delta progradation results in increasingly thicker beds (Reineck and Singh, 1980), whereas glacial recession results in lower sedimentation rates (Fleisher et al., 2003). Variances in rhythmite thickness can therefore result independent of external forcing. Ridge et al. (2012) also noted that prodeltaic varves may be difficult to correlate on a regional basis because of the influence of local processes.

Multiple depositional processes may also be contained within the annual boundaries delineating a single varve. In a study of Nicolay Lake, located on Cornwall Island in the Canadian High Arctic, Hambley and Lamoureux (2006) identified three subannual depositional layers found within the annual parameters that define a varve: (1) a basal layer deposited by sedimentation resulting from nival melt in the spring; (2) a layer resulting from hydrological events induced by precipitation, and (3) a layer resulting from sporadic mass wasting events such as turbidites or slumps. By comparing local weather station records with nival melt rhythmite thicknesses, Hambley and Lamoureux (2006) found a strong correlation between nival melt sedimentation and cumulative seasonal melt degree days. The combined measured thickness variations in meteoric-induced hydrological events and mass wasting events however, were demonstrated to be randomly variable and not associated with cumulative melt degree-days in a season, which may partially account for the inconclusive spectral analysis results of their study.

6.3. Robustness of the model

Spectral analysis investigations often invoke the use of two models to demonstrate that results are consistent (e.g. Andrews et al., 2010; Ojala et al., 2015). In the present study, the model that was chosen (Mann and Lees, 1996) was designed for, and has been demonstrated to work with, natural phenomena such as rhythmic laminations and tree-ring growth. Notwithstanding the designed intention of the model, the output may contain false-positive results (Mann and Lees, 1996). This study however, is predominantly concerned with relative comparisons among similar deposits, and therefore a single model was deemed sufficient. Moreover, the MTM results were shown to be consistent with the results of Hughes et al. (2003), who used the Maximum Entropy Method with the same data. Another issue facing spectral analysis modelling is that of persistence, which relates to zones (subsets) of anomalous data that may influence the results of the entire dataset. In geological terms, this may be represented by a period of extended warmth leading to rhythmites that are generally thicker than those that are predominant in the record. The present study also utilized small datasets, which (under the assumption of annual deposition) limited the output potential to decadal-scale results. Although this allowed for the possibility of finding short-term solar cycles related to sunspot activity (11 yr and 22 yr periodicities), none were consistently identified. This result is consistent with those of Zhao and Feng (2015), who found no connection between short-term solar cycles (11 and 22 yr periodicities) and local temperatures in modern Antarctica.

Conclusions

Rhythmic couplets of the upper Gowganda Formation preserve a high-resolution record of climatic variance during the Paleoproterozoic. MTM spectral analysis using time-series from four rhythmic couplet records measured in the field at two outcrop locations consistently revealed periodicities in the thickness of the rhythmites with periods of ca. 3 couplets per cycle. Modern annual climatic cycles such as the QBO and the ENSO also display periodicities of 3 years. Longer term periodicities of 3.0-14.3 couplets, 22.8 couplets, 30.1-31.0 couplets and 56.9 couplets were also preserved, but none of these results were represented in all four rhythmite records. The lack of consistency among all four rhythmite records for periodicities greater than 3 couplets may be the result of variations in the varve formation process or the depositional environment, gaps in the varve chronology, or errors attributed to the model. If climatic cycles similar to the QBO and the ENSO were operational during the Paleoproterozoic, the rhythmic couplets probably represent annual deposits (i.e. varves), and thus preserve a detailed record of Paleoproterozoic climate.

Acknowledgements

The authors gratefully acknowledge the provision of the raw data from Hughes et al. (2003) by G. Hughes., as well as discussions held with Dr. K. Tiampo who suggested the use of the MTM toolkit and provided access to Linux-based computers. This work was financially supported by an Academic Development Fund Major Grant provided to P. Corcoran by the University of Western Ontario.

References

Agterberg, F.P. and Banerjee, I., 1969. Stochastic model for the deposition of varves in glacial Lake Barlow-Ojibway, Ontario, Canada. Can. J. Earth Sci. 6, 625-652.

Andrews, S.D., Trewin, N.H., Hartley, A.J., Weedon, G.P., 2010. Solar variance recorded in lacustrine deposits from the Devonian and Proterozoic of Scotland. J. Geol. Soc. 167, 847-856.

Antevs, E., 1925. Retreat of the last ice sheet in eastern Canada. Geol. Surv. Can. Mem. 146, 142pp.

Archer, A.W., Kvale, E.P., Johnson, H.R., Williams, G., 1990. Discussion on Late Precambrian tidal rhythmites in South Australia and the history of the Earth’s rotation-reply. J. Geol. Soc. 147, 401-407.

Archer, A.W., Kuecher, G.J., Kvale, E.P., 1995. The role of tidal-velocity asymmetries in the deposition of silty tidal rhythmites (Carboniferous, Eastern Interior Coal Basin, U.S.A.). J. Sediment. Res. 65, 408-416.

Baldwin, M.P., Gray, L.J., Dunkerton, T.J., Hamilton, K., Haynes, P.H., Randel, W.J., Holton, J.R., Alexander, M.J., Hirota, I., Horinouchi, T., Jones, D.B.A., Kinnersley, J.S., Marquardt, C., Sato, K., Takahashi, M., 2001. The quasi-biennial oscillation. Rev. Geophys. 39, 179-229.

Bennett, G., 2006. The Huronian Supergroup Between Sault Ste. Marie and Elliot Lake. Institute on Lake Superior Geology, 74pp.

Bramlette, M.N., 1946. The Monterey Formation of California and the origin of its siliceous rocks. U.S. Geol. Surv. Prof. Pap. 212, 57pp.

Breckenridge, A., 2007. The Lake Superior varve stratigraphy and implications for eastern Lake Agassiz outflow from 10,700 to 8900 cal ybp (9.5–8.0 ^{14}C ka). Palaeogeogr. Palaeoclimatol. Palaeoecol. 246, 45-61.

Chan, M.A., Kvale, E.P., Archer, A.W., Sonett, C.P., 1994. Oldest direct evidence of lunar-solar tidal forcing encoded in sedimentary rhythmites, Proterozoic Big Cottonwood Formation, central Utah. Geology 22, 791-794.

Corfu, F., Andrews, A., 1986. A U-Pb age for mineralized Nipissing diabase, Gowganda, Ontario. Can. J. Earth Sci. 23, 107-109.

de Alvarenga, C.J., Trompette, R., 1992. Glacially influenced sedimentation in the later Proterozoic of the Paraguay Belt (Mato Grosso, Brazil). Palaeogeogr. Palaeoclimatol. Palaeoecol. 92, 85-105.

De Geer, G., 1912. Geochronology of the last 12,000 years. In: 11th International Geological Congress (1910), Stockholm, Sweden, vol. 1, pp. 241-253.

Delaney, C., 2005. Seasonal controls on deposition of Late Devensian glaciolacustrine sediments, central Ireland. In: Hambrey, M.J., Christofferson, P., Glasser, N.F., Hubbard, B. (Eds.), Glacial Sedimentary Processes and Products, Int. Assoc. Sedimentologists Spec. Pub. 39, 149-163.

Eyles, N., 2008. Glacio-epochs and the supercontinent cycle after ∼ 3.0 Ga: Tectonic boundary conditions for glaciation. Palaeogeogr. Palaeoclimatol. Palaeoecol. 258, 89-129.

Fleisher, P.J., Bailey, P.K., Cadwell, D.H., 2003. A decade of sedimentation in ice-contact, proglacial lakes, Bering Glacier, AK. Sediment. Geology 160, 309-324.

Freeman, E. B., 1978. Geological Highway Map, Southern Ontario; Ont. Geol. Surv., Map 2418

Godsey, H.S., Moore, T.C., Rea, D.K., Shane, L.C.K., 1999. Post-Younger Dryas seasonality in the North American midcontinent region as recorded in Lake Huron varved sediments. Can. J. Earth Sci. 36, 533-547.

Hambley, G.W., Lamoureux, S.F., 2006. Recent summer climate recorded in complex varved sediments, Nicolay Lake, Cornwall Island, Nunavut, Canada. J. Paleolimnol. 35, 629-640.

Holm, D.K., Van Schmus, W.R., MacNeill, L.C., Boerboom, T.J., Schweitzer, D., Schneider, D., 2005. U-Pb zircon geochronology of Paleoproterozoic plutons from the northern midcontinent, USA: Evidence for subduction flip and continued convergence after geon 18 Penokean orogenesis. Geol. Soc. Am. Bull. 117, 259-275.

Howe, T.S., 2015. Investigating potential climatic cycles in glacially-influenced rhythmites of the upper Gowganda Formation using geochemical, sedimentological and spectral analyses. Master's Thesis, Western University.

Hughes, G.B., Giegengack, R., Kritikos, H.N., 2003. Modern spectral climate patterns in rhythmically deposited argillites of the Gowganda Formation (Early Proterozoic), southern Ontario, Canada. Ear. Plan. Sci. Lett. 207, 13-22.

Klein, G.D., 1971. A sedimentary model for determining paleotidal range. Geol. Soc. Am. Bull. 82, 2585-2592.

Krogh, T., Davis, D., Corfu, F., 1984. Precise U-Pb zircon and baddeleyite ages for the Sudbury area, in: Pye, E.G., Naldrett, A.J., Giblin, P.E. (Eds.), The Geology and Ore Deposits of the Sudbury Structure, Ont. Geol. Surv., Spec., Vol. 1, pp. 431–446.

Lindsey, D.A., 1969. Glacial sedimentology of the Precambrian Gowganda Formation, Ontario, Canada. Geol. Soc. Am. Bull. 80, 1685-1702.

Long, D.G., 1978. Depositional environments of a thick Proterozoic sandstone: the (Huronian) Mississagi Formation of Ontario, Canada. Can. J. Earth Sci. 15, 190-206.

Long, D.G., 2004. The tectonostatigraphic evolution of the Huronian basement and the subsequent basin fill: geological constraints on impact models of the Sudbury event. Precambrian Res. 129, 203-223.

Long, D.G., 2009. The Huronian Supergroup, in: Rousell, D.H. and Brown, G.H. (Eds.), A Field Guide to the Geology of Sudbury, Ontario, Ont. Geol. Surv., Open File Rep. 6243, pp. 14-30.

Mann, M.E., Lees, J.M., 1996. Robust estimation of background noise and signal detection in a climatic time series. Clim. Change 33, 409-445.

Martins-Neto, M.A., Pedrosa-Soares, A.C., Lima, S.A.D.A., 2001. Tectono-sedimentary evolution of sedimentary basins from Late Paleoproterozoic to Late Neoproterozoic in the Sao Francisco craton and Araçuaı fold belt, eastern Brazil. Sediment. Geol. 141, 343-370.

Mazumder, R., 2004. Implications of lunar orbital periodicity from the Chaibasa tidal rhythmite (India) of late Paleoproterozoic age. Geology 32, 841-844.

Moore Jr, J.M., Thompson, P.H., 1980. The Flinton Group: a late Precambrian metasedimentary succession in the Grenville Province of eastern Ontario. Can. J. Earth Sci. 17, 1685-1707.

Mustard, P., Donaldson, J., 1987. Early Proterozoic ice-proximal glaciomarine deposition: the lower Gowganda Formation at Cobalt, Ontario, Canada. Geol. Soc. Am. Bull. 98, 373-387.

Ojala, A.E.K., Francus, P., Zolitschka, B., Besonen, M., & Lamoureux, S.F., 2012. Characteristics of sedimentary varve chronologies–a review. Quat. Sci. Rev., 43, 45-60.

Palonen, P., 1973. Paleogeography of the Mississagi Formation and lower Huronian cyclicity, in: Young, G.M. (Ed.), Huronian Stratigraphy and Sedimentation, Geol. Assoc. Canada Spec. Pap. 12, pp. 157-167.

Rainbird, R.H., 1985. Sedimentology and geochemistry of the Firstbrook Member of the Gowganda Formation in the eastern Cobalt Basin, M.Sc. thesis, Carleton University, Ottawa, Ont., Canada, 157 pp.

Rasmussen, B., Bekker, A. and Fletcher, I.R., 2013. Correlation of Paleoproterozoic glaciations based on U–Pb zircon ages for tuff beds in the Transvaal and Huronian Supergroups. Earth Planet. Sci. Lett. 382, 173-180.

Reineck, H.E., Singh, I.B., 1972. Genesis of laminated sand and graded rhythmites in storm-sand layers of shelf mud. Sedimentol. 18, 123-128.

Reineck, H.E., Singh, I.B., 1980. Depositional Sedimentary Environments: With Reference to Terrigenous Clastics. Springer-Verlag, Berlin, 549pp.

Ridge, J.C., Balco, G., Bayless, R.L., Beck, C.C., Carter, L.B., Dean, J.L., Voytek, E.B., Wei, J.H., 2012. The new North American Varve Chronology: A precise record of southeastern Laurentide Ice Sheet deglaciation and climate, 18.2-12.5 kyr BP, and correlations with Greenland ice core records. Am. J. Sci. 312, 685-722.

Rittenour, T.M., Brigham-Grette, J., Mann, M.E., 2000. El Niño-like climate teleconnections in New England during the late Pleistocene. Science 288, 1039–1042.

Tang, H., Chen, Y., 2013. Global glaciations and atmospheric change at ca. 2.3 Ga. Geosci. Front. 4, 583-596.

Thomson, D.J., 1982. Spectrum estimation and harmonic analysis. Proc IEEE 70: 1055-1096.

Weedon, G.W., 2003. Time-Series Analysis and Cyclostratigraphy: Examining stratigraphic records of environmental cycles, Cambridge University Press, UK, 259pp.

Williams, G., 1981. Sunspot periods in the late Precambrian glacial climate and solar–planetary relations. Nature 291, 624-628.

Williams, G., 1985. Solar affinity of sedimentary cycles in the late Precambrian Elatina Formation. Australian J. Physics 38, 1027-1044.

Williams, G.E., 1989. Late Precambrian tidal rhythmites in South Australia and the history of the Earth's rotation. J. Geol. Soc. 146, 97-111.

Williams, G.E., 1991. Upper Proterozoic tidal rhythmites, South Australia: sedimentary features, deposition, and implications for the earth’s paleorotation. In: Smith, D.G., Reinson, G.E., Zaitlin, B.A., Rahmani, R.A. (Eds.), Clastic Tidal Sedimentology, Can. Soc. Pet. Geol. Mem. 16, 161-177.

Williams, G.E., 2000. Geological constraints on the Precambrian history of Earth's rotation and the Moon's orbit. Rev. Geophys. 38, 37-59.

Willingham, T.O., Nagy, B., Nagy, L.A., Krinsley, D.H., Mossman, D.J., 1985. Uranium-bearing stratiform organic matter in paleoplacers of the lower Huronian Supergroup, Elliot Lake-Blind River region, Canada. Can. J. Earth Sci. 22, 1930-1944.

Young, G.M., 1970. An extensive early Proterozoic glaciation in North America? Palaeogeogr. Palaeoclimatol. Palaeoecol. 7, 85-101.

Young, G.M., 2013. Climatic catastrophes in Earth history: two great Proterozoic glacial episodes. Geol. J. 48, 1-21.

Young, G.M., Nesbitt, H.W., 1985. The Gowganda Formation in the southern part of the Huronian outcrop belt, Ontario, Canada: Stratigraphy, depositional environments and regional tectonic significance. Precambrian Res. 29, 265-301.

Young, G.M., Long, D.G.F., Fedo, C.M., Nesbitt, H.W., 2001. Paleoproterozoic Huronian basin: product of a Wilson cycle punctuated by glaciations and a meteorite impact. Sediment. Geol. 141, 233-254.

Zhao, X.H., Feng, X.S., 2015. Correlation between solar activity and the local temperature of Antarctica during the past 11,000 years. J. Atmos. Sol. Terr. Phys. 122, 26-33.

Figure Captions

Figure 1: Distribution of the Huronian Supergroup in Ontario, Canada. The Huronian Supergroup comprises the eastern section of the Southern Province, and is divided into three regions: the Bruce Mines/Elliot Lake area, the Espanola/Whitefish Falls area and the Cobalt area. The Flack Lake fault and the Murray fault zone (dashed lines) indicate contemporaneous down-to-basin faulting. Map modified from Freeman (1978) and Young et al. (2001)

Figure 2: Generalized stratigraphic section of the Huronian Supergroup. Note the repeating cycles of conglomerate overlain by siltstone or limestone, overlain by sandstone in each of the Hough Lake, Quirke Lake and Cobalt groups. The informal Flack Lake Group serves to separate the non-cyclical Gordon Lake and Bar River formations from the Cobalt Group (after Long, 2004).

Figure 3: Locations of studied outcrops in the Bruce Mines/Elliot Lake study area. Outcrop A also represents the location of the Hughes et al. (2003) study.

Figure 4: Characteristics of the rhythmites studied. A: Photograph of an approximately 4 m thick section of Outcrop A. B: Photograph of partial rhythmite sequence from Outcrop A, which locally contains granule- to boulder-size dropstones. C: Rhythmites at Outcrop B. Student is approximately 1.8 m tall. D: Photograph of partial rhythmite sequence at Outcrop B, which does not contain dropstones. Distance between tape markings is 30 cm.

Figure 5: (Bottom) Thickness of the 229 couplets that compose the lower set of measurements from Outcrop A. (Top) Thickness of the 585 couplets that compose the upper set of measurements from Outcrop A.

Figure 6: (Bottom) Thickness of the 216 couplets that compose the lower set of measurements from Outcrop B. (Top) Thickness of 119 couplets that compose the upper set of measurements from Outcrop B.

Figure 7: Spectral analysis results using the method of Mann and Lees (1996) for the rhythmite measurements of Hughes et al. (2003) with median, and 90%, 95% and 99% confidence interval bands. Quasi-periodic cycles with periods ranging from 2.3 to 13.3 couplets are shown. A harmonic cycle of period 2.7 couplets is indicated by the open rectangle.

Figure 8: (Bottom) Spectral analysis results using the method of Mann and Lees (1996) for the lower rhythmite measurements from Outcrop A with median, and 90%, 95% and 99% confidence interval bands. Quasi-periodic cycles with periods ranging from 2.2 to 9.2 couplets are shown. (Top) Spectral analysis results using the method of Mann and Lees (1996) for the upper rhythmite measurements from Outcrop A with median, and 90%, 95% and 99% confidence interval bands. Quasi-periodic cycles with periods ranging from 2.3 to 56.9 couplets are shown. A harmonic cycle of about 2.5 couplets is indicated by an open rectangle.

Figure 9: (Bottom) Spectral analysis results using the method of Mann and Lees (1996) for the lower rhythmite measurements from Outcrop B with median, and 90%, 95% and 99% confidence interval bands. Quasi-periodic cycles with periods ranging from 2.3 to 30.1 couplets

are shown. A harmonic cycle with a period of about 2.8 couplets is indicated by the open rectangle. (Top) Spectral analysis results using the method of Mann and Lees (1996) for the upper rhythmite measurements from Outcrop B with median, and 90%, 95% and 99% confidence interval bands. Quasi-periodic cycles with a period ranging from 2.9 to 6.9 couplets are shown.

Figures

Figure 1

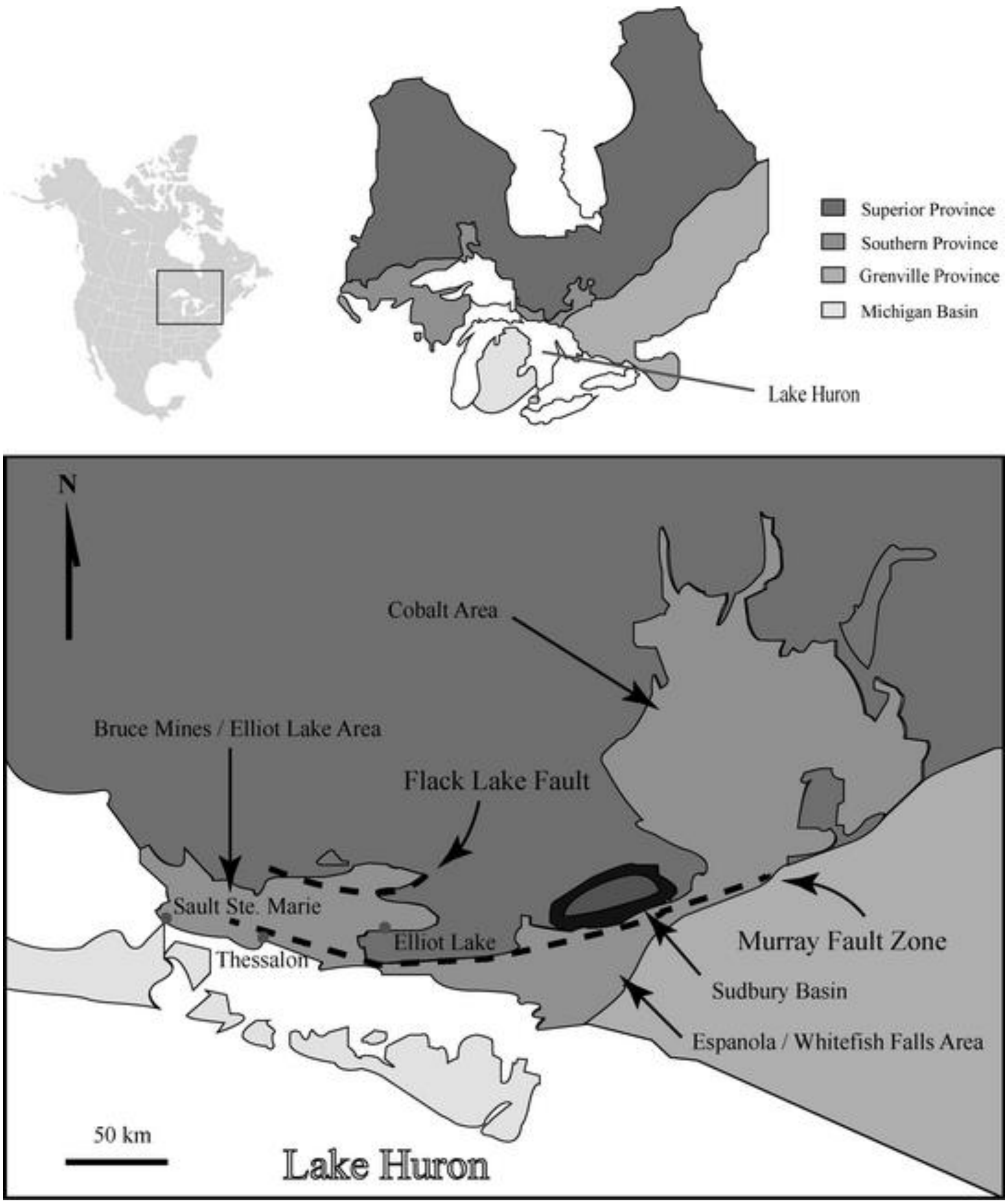

542 Figure 2

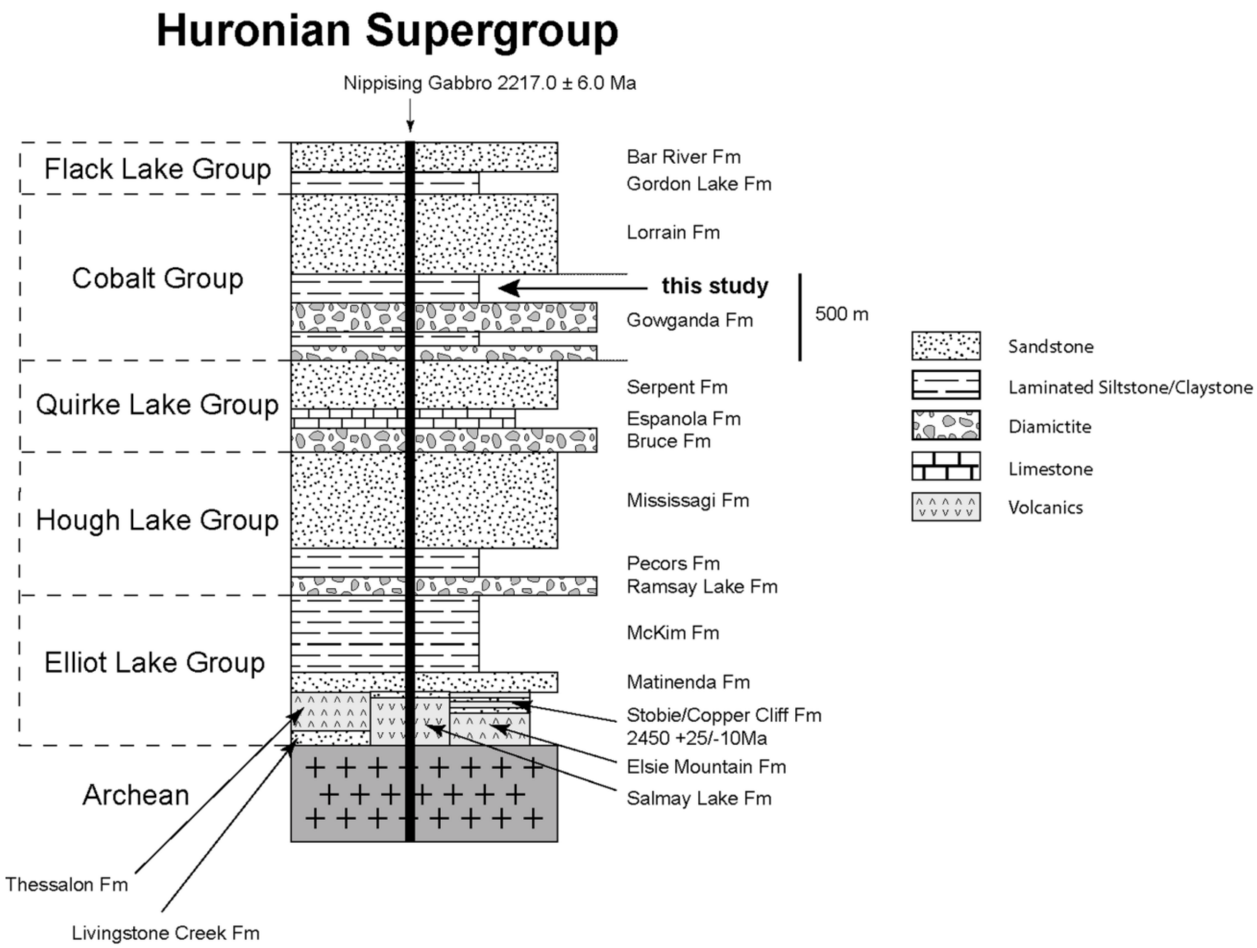

543

544

Figure 3

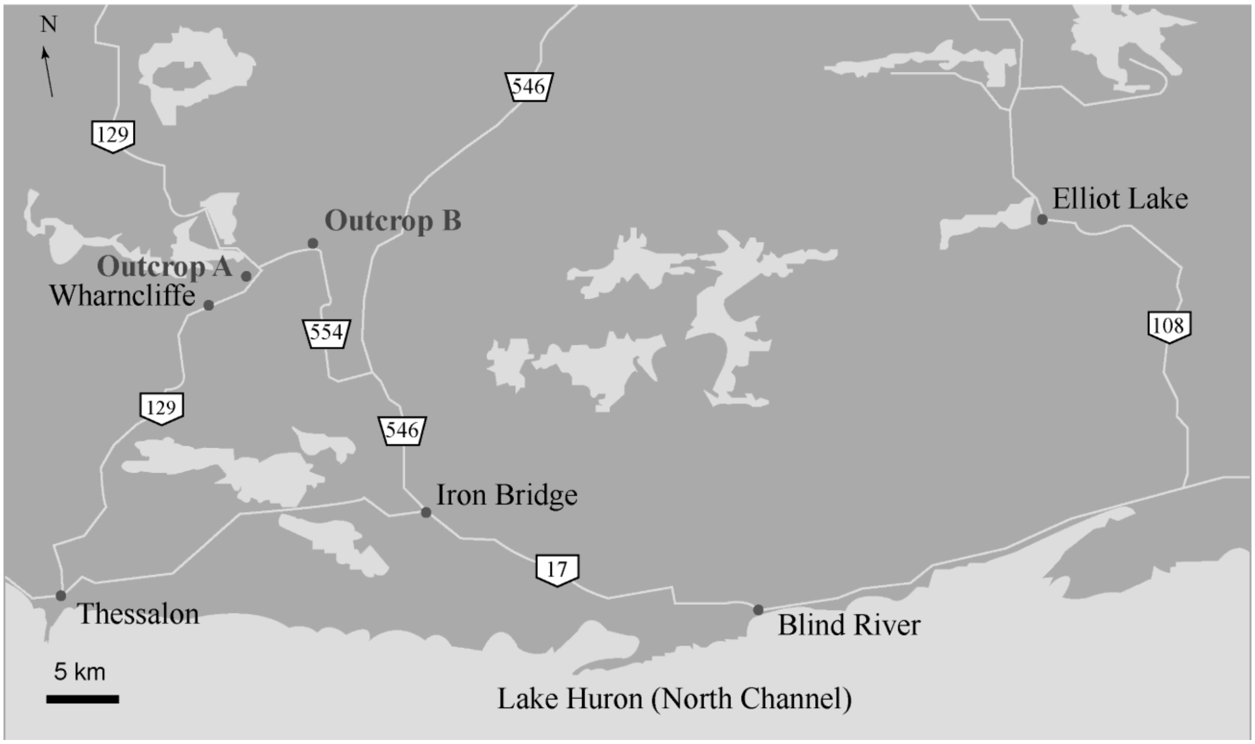
N
546
129
Outcrop B
Outcrop A
Wharncliffe
554
129
546
Iron Bridge
17
Elliot Lake
108
Thessalon
Blind River
5 km
Lake Huron (North Channel)

Figure 4

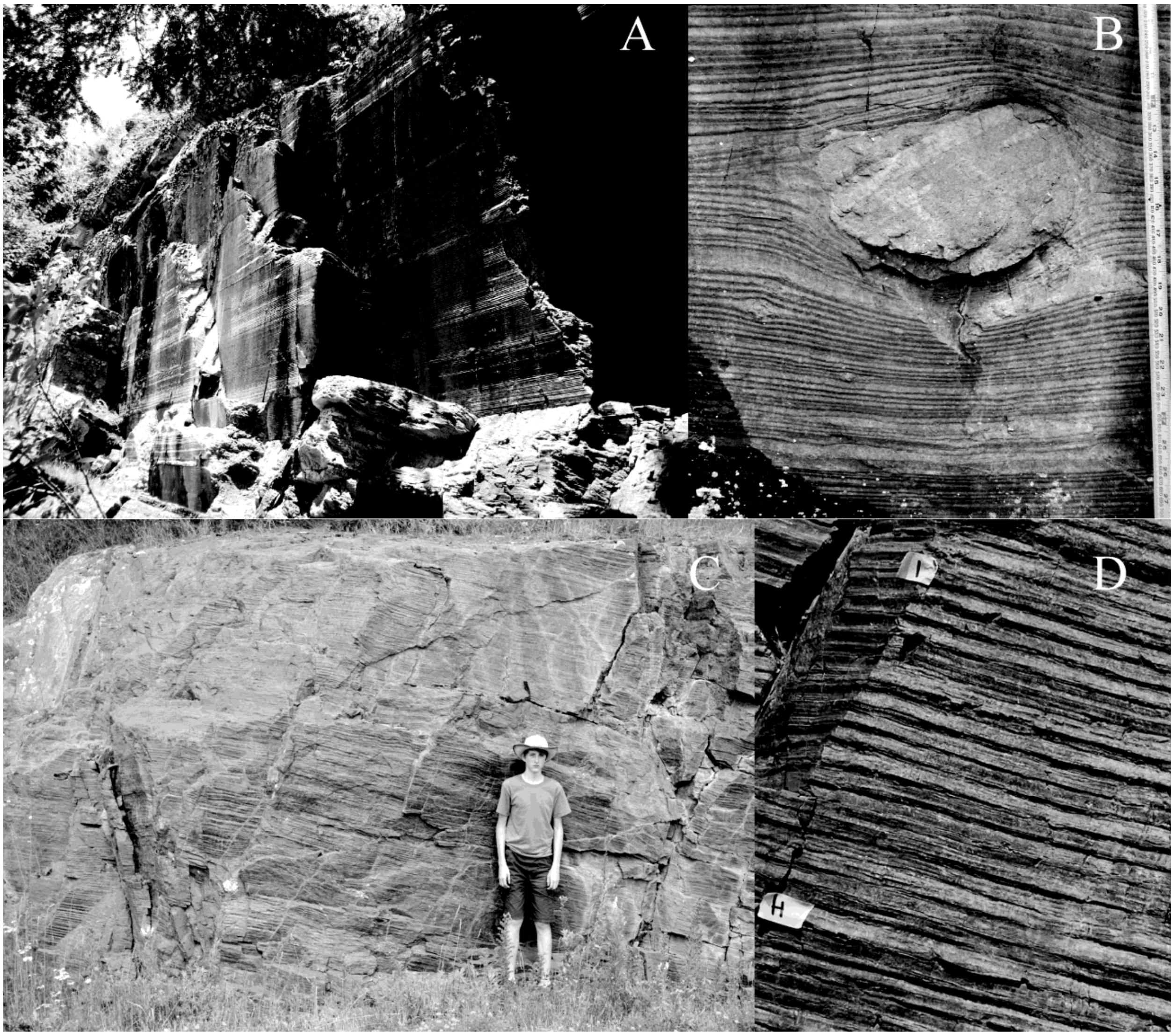

Figure 5

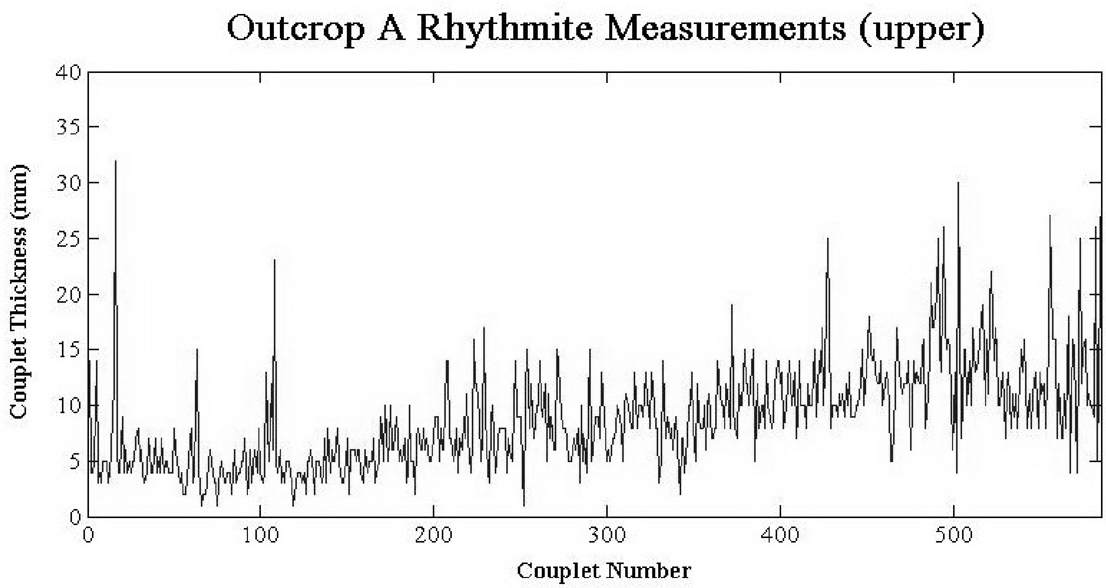
Outcrop A Rhythmite Measurements (upper)
Couplet Thickness (mm)
Couplet Number
0
5
10
15
20
25
30
35
40
100
200
300
400
500

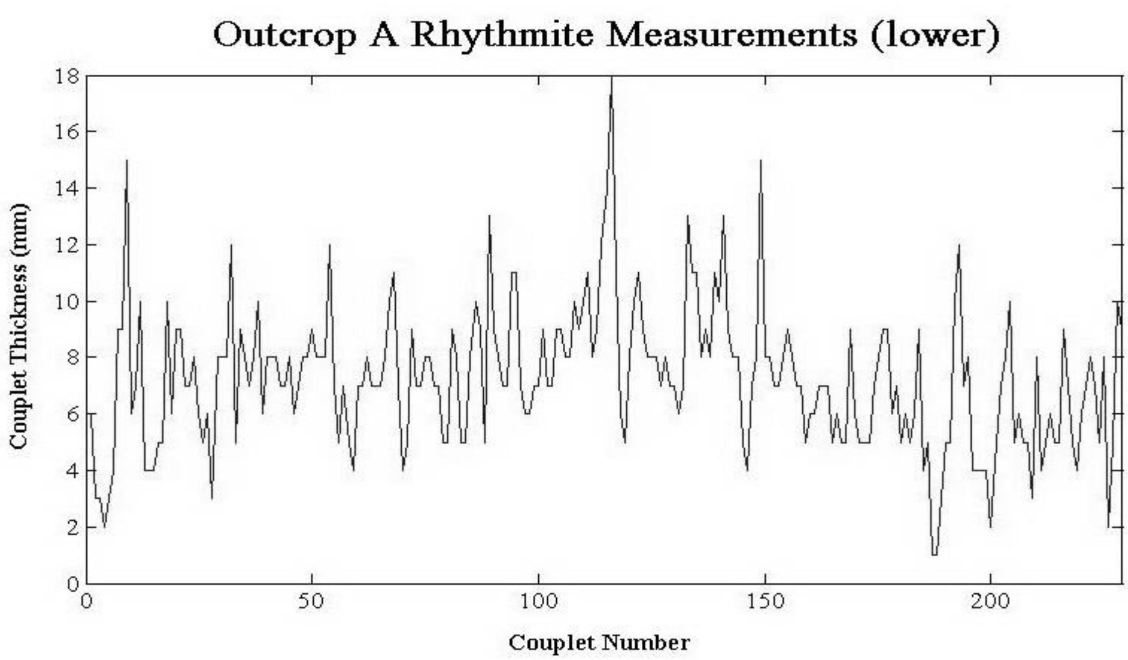
Outcrop A Rhythmite Measurements (lower)
Couplet Thickness (mm)
Couplet Number
0
2
4
6
8
10
12
14
16
18
50
100
150
200

Figure 6

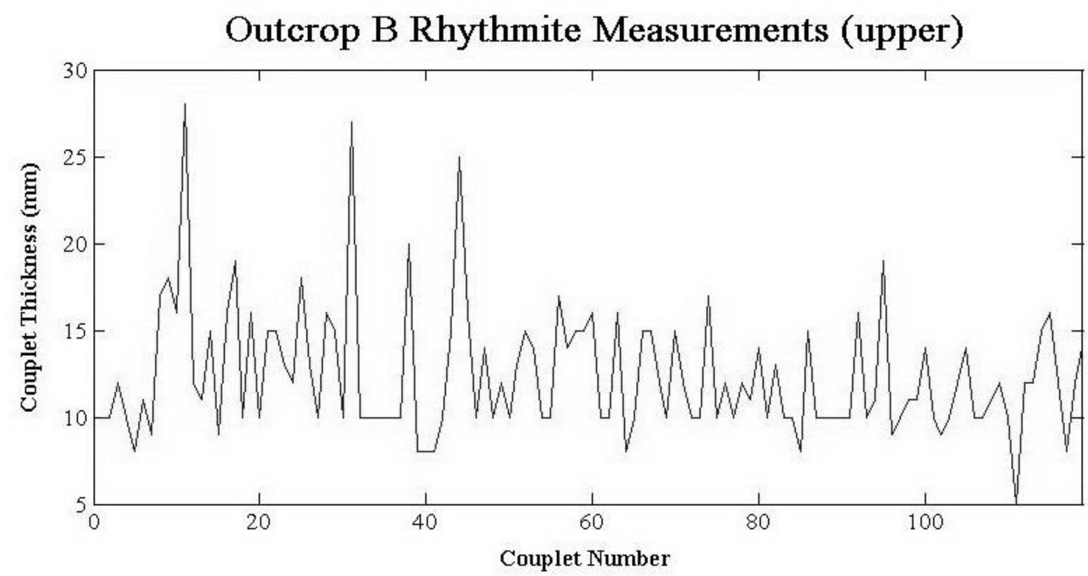
Outcrop B Rhythmite Measurements (upper)
Couplet Thickness (mm)
Couplet Number
30
25
20
15
10
5
0
20
40
60
80
100

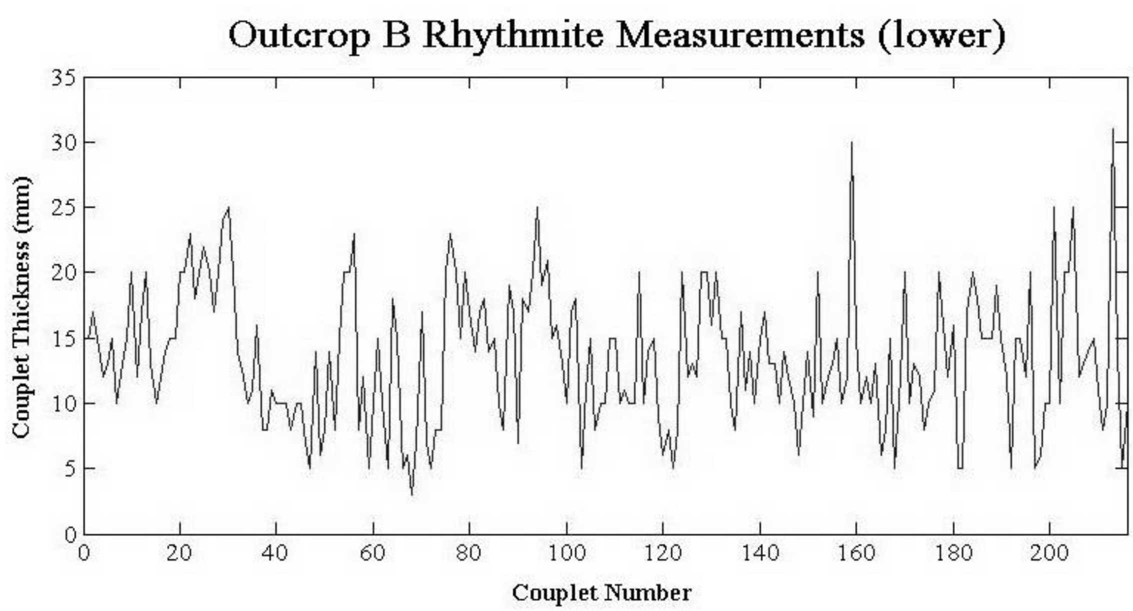
Outcrop B Rhythmite Measurements (lower)
Couplet Thickness (mm)
Couplet Number
35
30
25
20
15
10
5
0
0
20
40
60
80
100
120
140
160
180
200

Figure 7

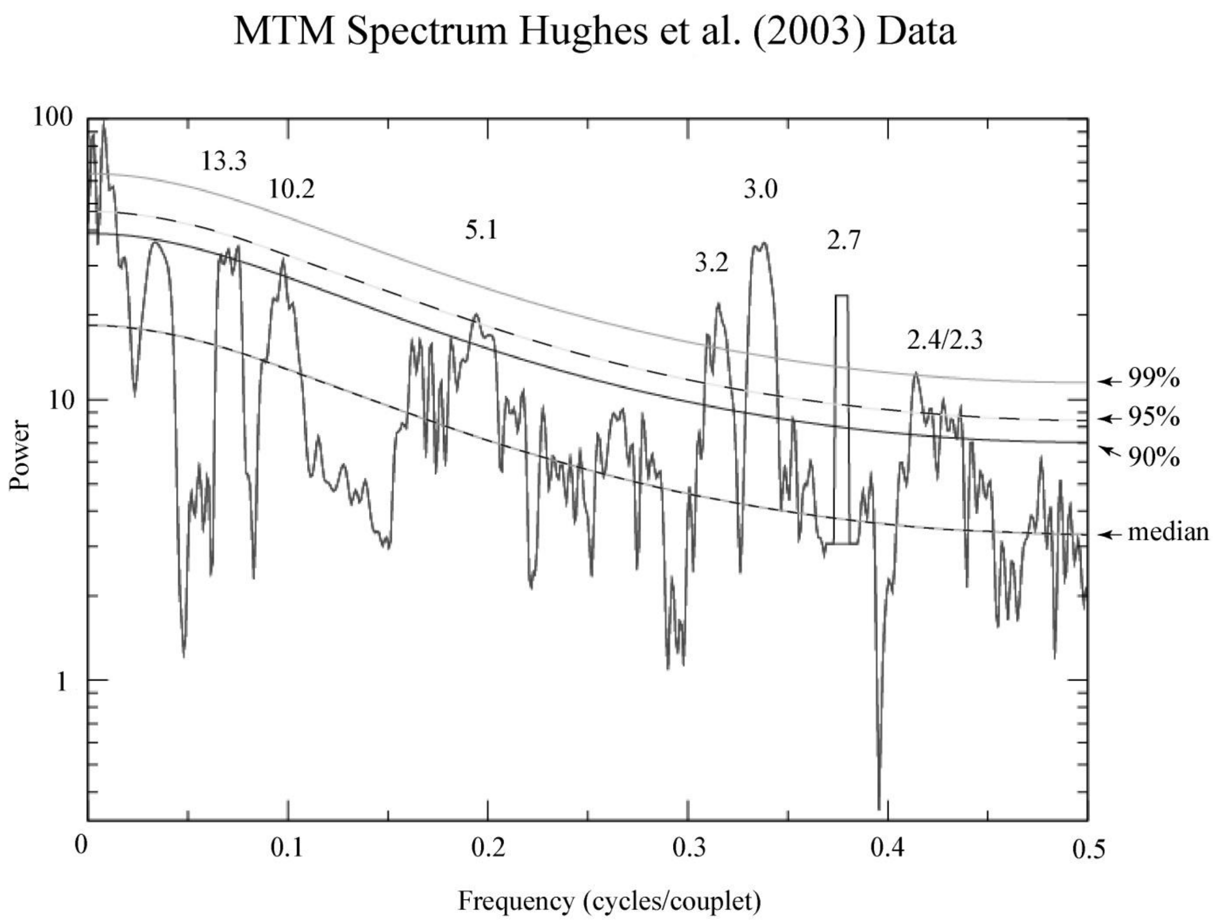
MTM Spectrum Hughes et al. (2003) Data
100
10
1
Power
0
0.1
0.2
0.3
0.4
0.5
Frequency (cycles/couplet)
13.3
10.2
5.1
3.2
3.0
2.7
2.4/2.3
99%
95%
90%
median

Figure 8

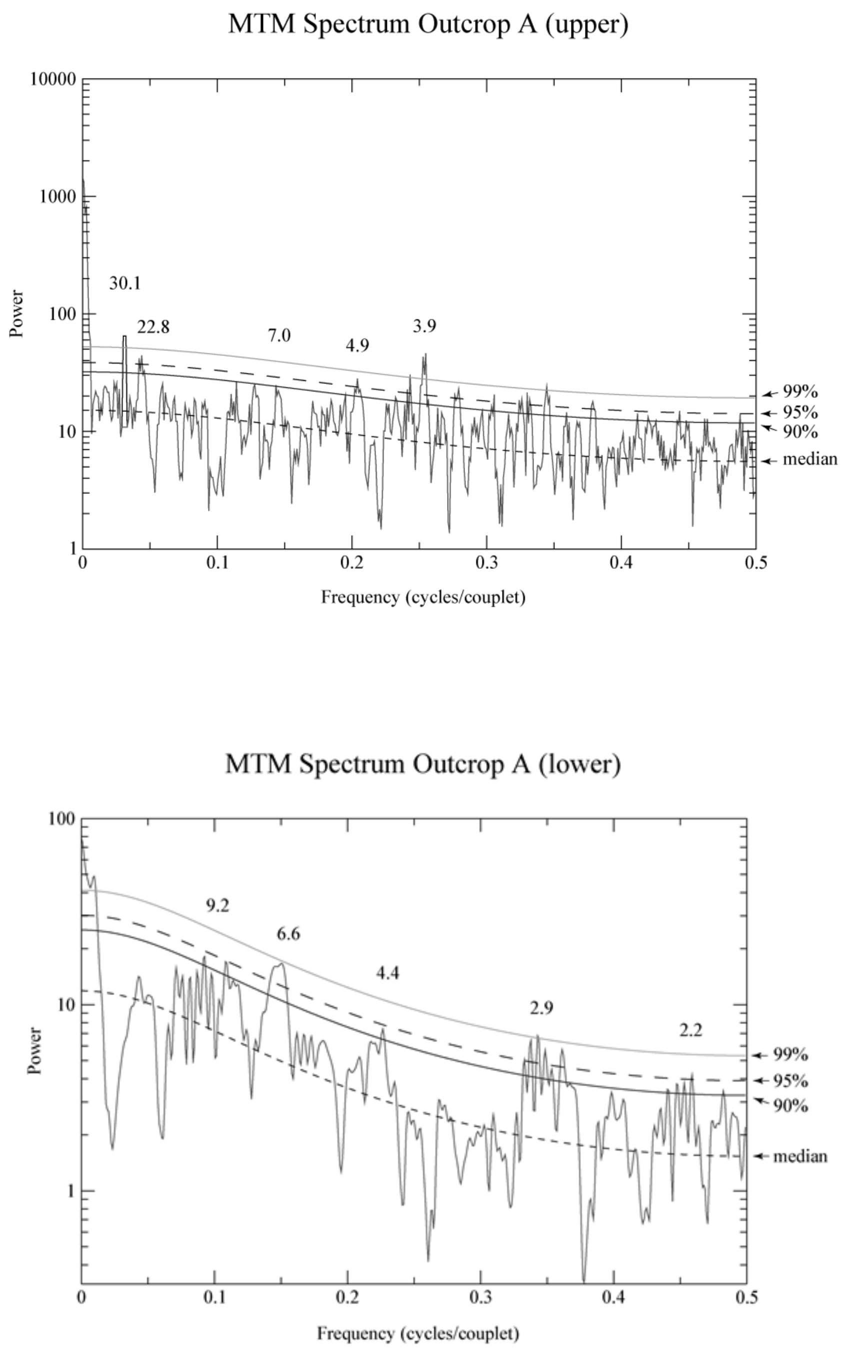
MTM Spectrum Outcrop A (upper)
Power
Frequency (cycles/couplet)
30.1
22.8
7.0
4.9
3.9
99%
95%
90%
median
MTM Spectrum Outcrop A (lower)
Power
Frequency (cycles/couplet)
9.2
6.6
4.4
2.9
2.2
99%
95%
90%
median

Figure 9

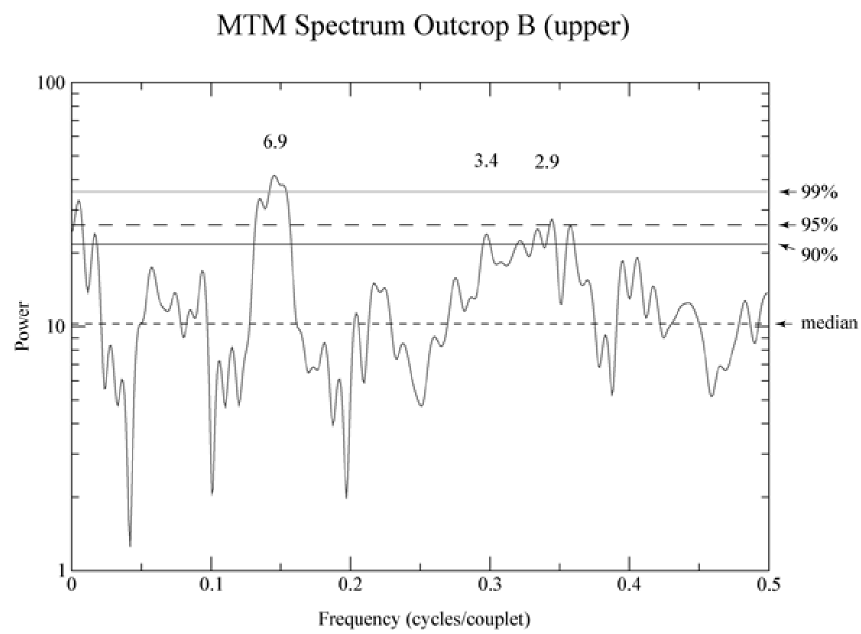
MTM Spectrum Outcrop B (upper)
Power
Frequency (cycles/couplet)
6.9
3.4
2.9
99%
95%
90%
median

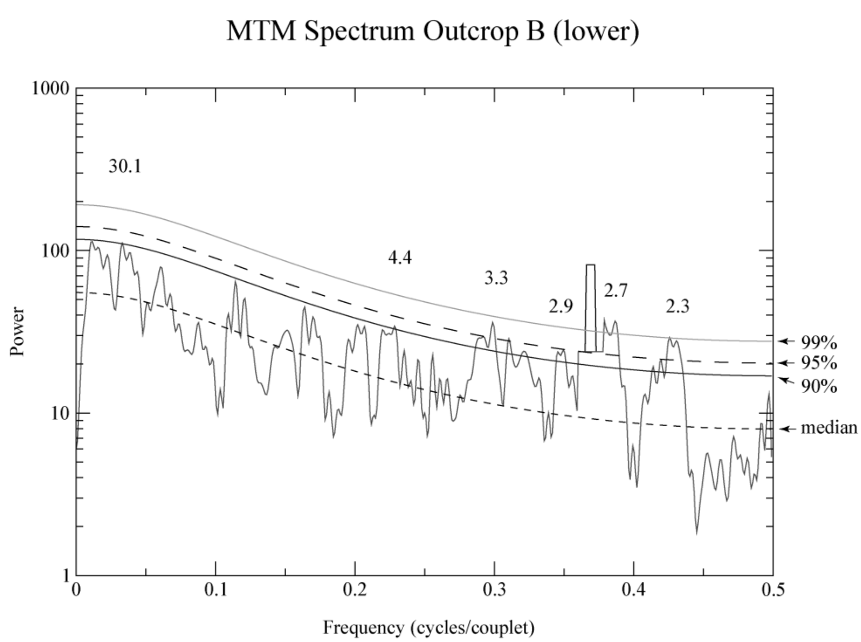
MTM Spectrum Outcrop B (lower)
Power
Frequency (cycles/couplet)
30.1
4.4
3.3
2.9
2.7
2.3
99%
95%
90%
median

Table 1: Sedimentological characteristics of the upper Gowganda Formation in the study area (from Howe, 2015**)**

Lithofacies	Characteristics & Bedding Features	Mechanisms & Processes	Interpretation & Setting
Siltstone-Claystone (1-15 m) Siltstone layers: 1-4 mm Claystone layers: 1-30 mm	Dark green to dark gray, alternating siltstone-claystone beds; siltstone layers 1-2 mm thick increase to 3-4 mm thick up-section; claystone layers are 1-30 mm thick; granitic/gneissic pebble- to boulder-sized dropstones become less abundant up-section; local lenticular, pink, fine- to very fine-grained wavy sandstone beds of starved ripples; grain size and irregular, non-rhythmic bedding increase up-section.	Rhythmites represent recurring flux in transport energy: lower energy results in claystone layers, and higher energy results in siltstone layers. Dropstones represent ice-rafted debris. Lenticular sandstone beds resulted from irregular increase in transport energy during periods of intense precipitation or distal jökulhlaups (glacial lake outburst floods).	Distal deltaic deposits.
Conglomerate (3 cm)	Pink granitic granules and pebbles in a grey argillaceous matrix.	Planar laminated within siltstone-claystone lithofacies.	Iceberg-dumped debris.
Sandstone (10 cm)	Pink, massive, rippled contact with underlying and overlying claystone beds.	Reworked, locally available sand.	Delta front sand sheet associated with delta progradation.
Siltstone (2.7 m) Siltstone layers: 1-50 cm Mudstone layers: 0.5-10 cm	Siltstone beds 15-25 cm thick interbedded with rhythmic intervals of siltstone and mudstone; rhythmic sequences are 8-10 cm thick, and are composed of beds of siltstone averaging 1.5 cm thick and mudstone laminations up to 1 cm thick.	The intercalated siltstone and mudstone beds indicate variations in sedimentation rate, whereas thicker siltstone beds indicate a steady sedimentation rate.	Short term, possibly diurnal, stops and starts in glacial melting that could be associated with a cycle of freezing conditions at night and melting conditions during the day. Summer melt cycle resulted in continuous, silty sedimentation. Possible delta lobate deposit.
Wavy Mudstone (35 m)	Thin beds of wavy, parallel mudstone. Measured wavelengths between 1.6 and 4.5 m and 13-22 cm high.	Very fine grain size indicates low transport energy and greater distance from glacier.	Possible overbank or inner bay floor deposits influenced by waves.
Siltstone (7 m) Coarse-grained siltstone: 15-50 cm Fine-grained siltstone: 5-40 cm	Grey, thin, planar bedded, coarse- and fine-gained siltstone couplets that range from 3-31 mm thick.	Fluctuating current energy conditions; Increasingly rapid deposition is indicated up-section by flame structures in the fine-grained siltstone, and lenses in the coarse-grained siltstone layers.	Possible fluvial deposits that were transported to a medial delta front.

Table 2: Summary of spectral analysis results from this study, and the Hughes et al. (2003) study

Outcrop A (lower) n=229 *period (couplets)*	Outcrop A (upper) n=585 *period (couplets)*	Outcrop B (lower) n=216 *period (couplets)*	Outcrop B (upper) n=119 *period (couplets)*	Hughes (MTM)[2] n=256 *period (couplets)*	Hughes (published)[1] n=256 *period (couplets)*
	31	30.1			
	22.8			13.3	14.3
9.2	8.8			10.2	10.7, 9.9
6.6			6.9		6.1
4.4	3.0 - 4.9	3.3 - 4.4	3.0 - 3.4	3.0 - 3.2, 5.1	3.0 - 5.0
2.2 - 2.9	2.3 - 2.9	2.3 - 2.9	2.8 - 2.9	2.3 - 2.9	2.3 - 2.9

Results are shown for detected signal periods (in couplets).
Results from the Hughes et al. (2003) study as published[1], and as produced by the MTM Toolkit[2], are shown with this study's results.

Table 3: Comparison of this study with similar studies conducted in the Great Lakes region.

Study	**Deposits**	**ENSO**	**NAO**
Godsey et al. (1999)	Lake Huron sediments	3 - 7 years	n/a
Rittenour et al. (2000)	Lake Hitchcock sediments	3 - 7 years	n/a
Breckenridge (2007)	Lake Superior sediments	3 - 6 years	6 - 7 years
Hughes et al. (2003)	Gowganda Fm sediments	3 - 6 years	6 - 7 years
This study (2016)	Gowganda Fm sediments	3 - 6 years	6 - 7 years

If the period of deposition is interpreted to be one year then spectral signals in the 3 - 6 year range may result from oceanic oscillations similar to the El Niño Southern Oscillation (ENSO) and periods of 6 – 7 years may indicate the influence of an oceanic oscillation similar to the North Atlantic Oscillation (NAO).

Colour Images for On-line Publication Only

Figure 1

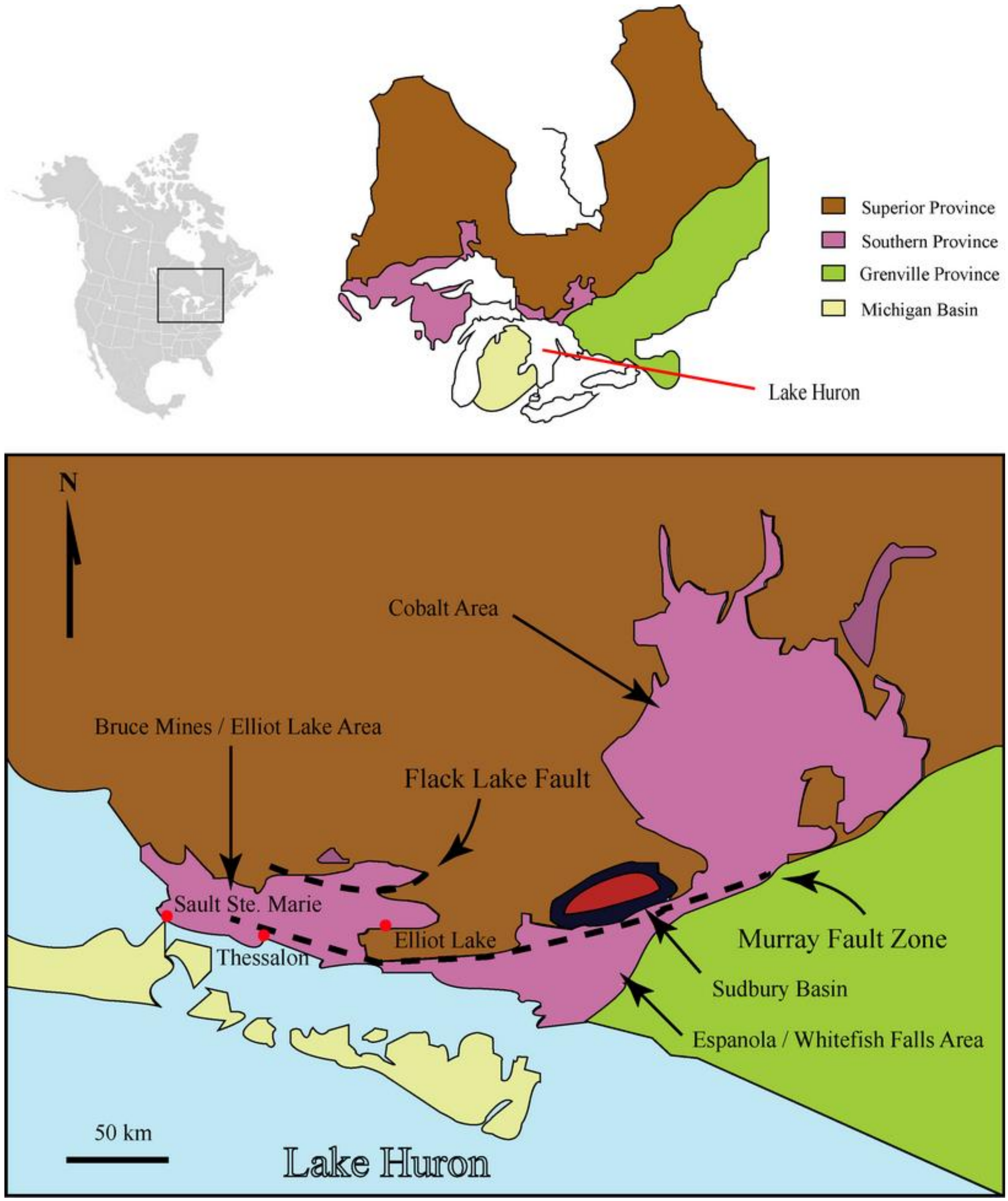
Superior Province
Southern Province
Grenville Province
Michigan Basin
Lake Huron
N
Cobalt Area
Bruce Mines / Elliot Lake Area
Flack Lake Fault
Sault Ste. Marie
Thessalon
Elliot Lake
Murray Fault Zone
Sudbury Basin
Espanola / Whitefish Falls Area
50 km
Lake Huron

Figure 2

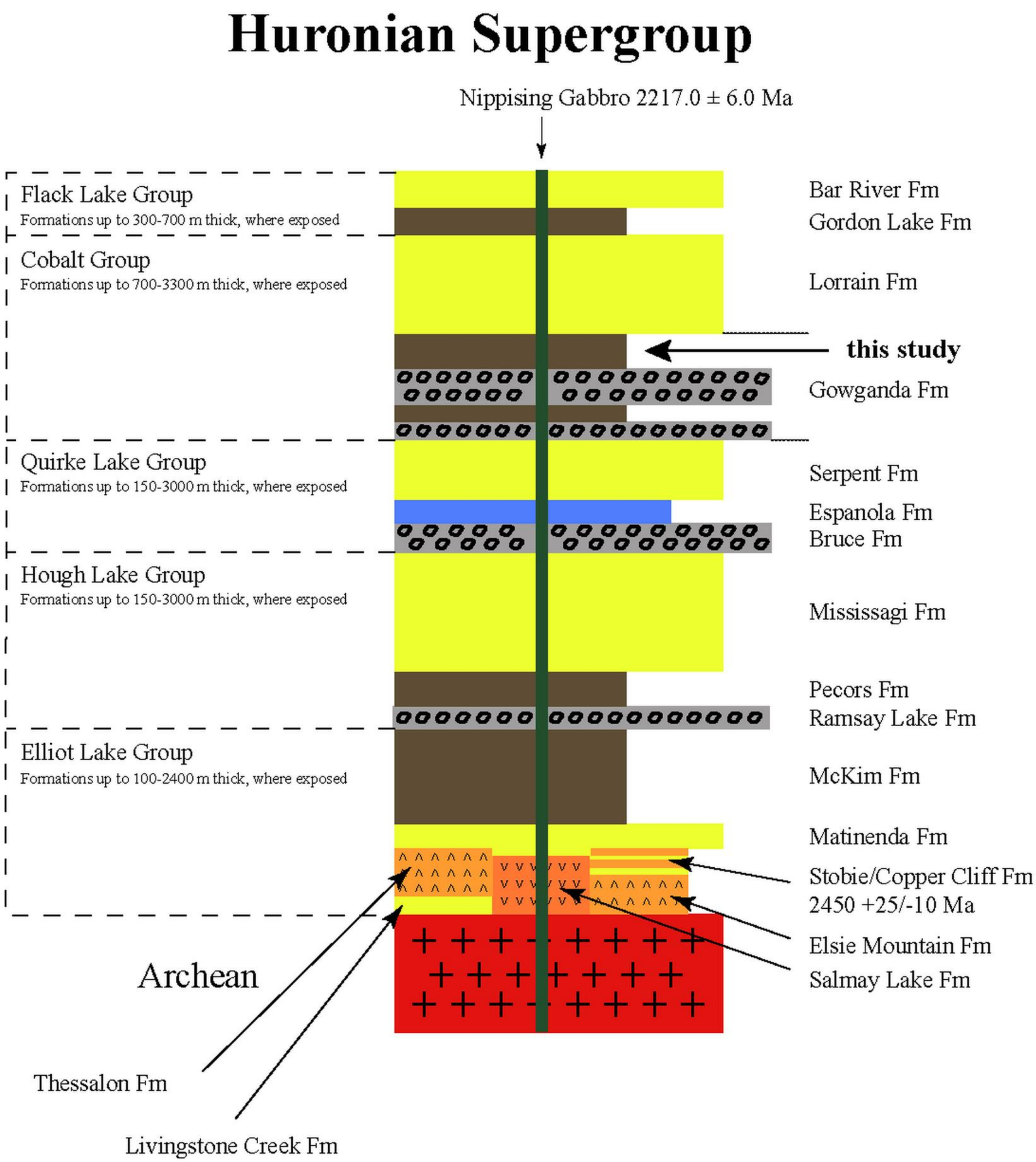
Huronian Supergroup
Nippising Gabbro 2217.0 ± 6.0 Ma
Flack Lake Group
Formations up to 300-700 m thick, where exposed
Cobalt Group
Formations up to 700-3300 m thick, where exposed
Quirke Lake Group
Formations up to 150-3000 m thick, where exposed
Hough Lake Group
Formations up to 150-3000 m thick, where exposed
Elliot Lake Group
Formations up to 100-2400 m thick, where exposed
Archean
Bar River Fm
Gordon Lake Fm
Lorrain Fm
this study
Gowganda Fm
Serpent Fm
Espanola Fm
Bruce Fm
Mississagi Fm
Pecors Fm
Ramsay Lake Fm
McKim Fm
Matinenda Fm
Stobie/Copper Cliff Fm
2450 +25/-10 Ma
Elsie Mountain Fm
Salmay Lake Fm
Thessalon Fm
Livingstone Creek Fm

Figure 3


N
546
129
Outcrop B
Outcrop A
Elliot Lake
554
108
129
546
Iron Bridge
17
Thessalon
Blind River
5 km
Lake Huron (North Channel)

Figure 4

Figure 5

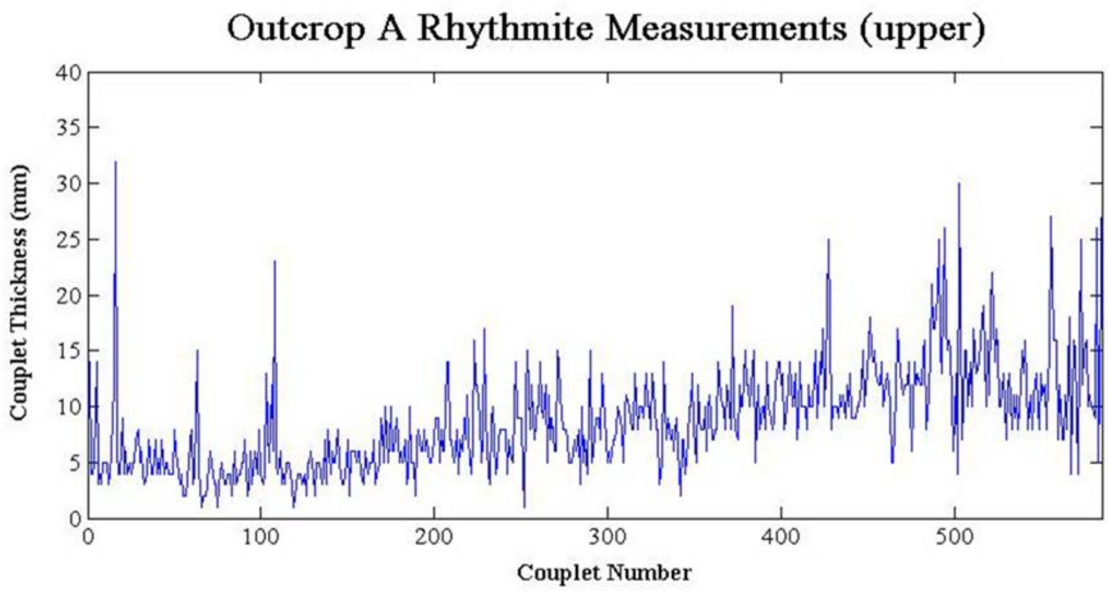
Outcrop A Rhythmite Measurements (upper)
Couplet Thickness (mm)
Couplet Number
0
5
10
15
20
25
30
35
40
100
200
300
400
500

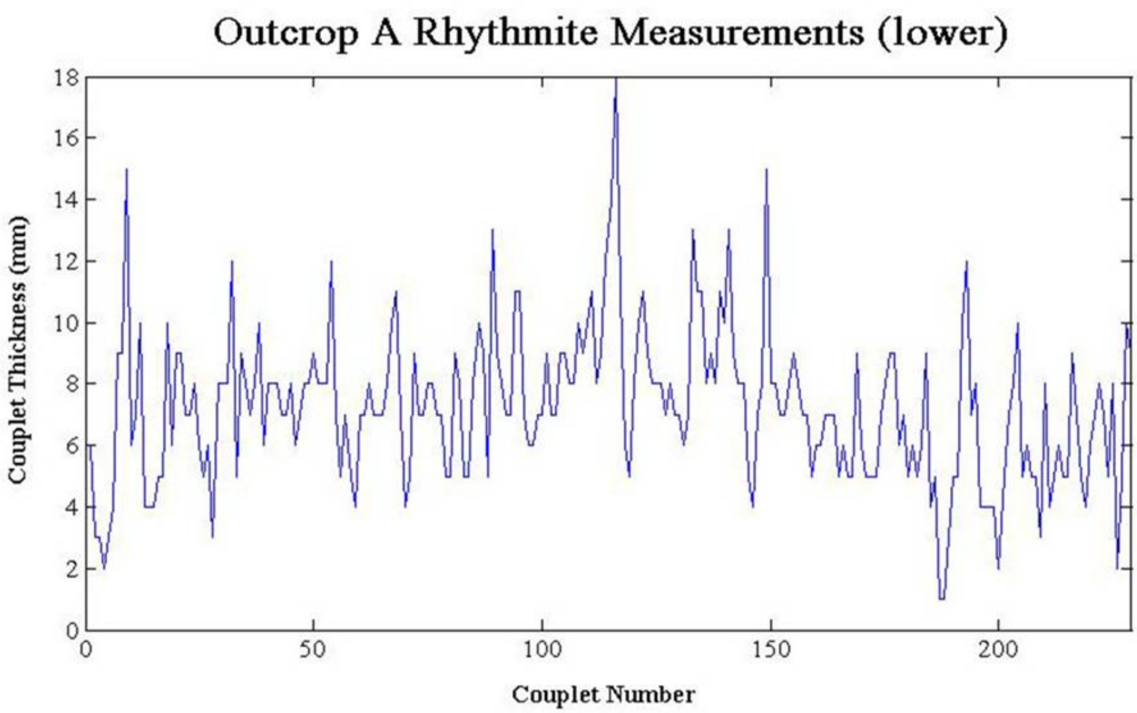
Outcrop A Rhythmite Measurements (lower)
Couplet Thickness (mm)
Couplet Number
0
2
4
6
8
10
12
14
16
18
50
100
150
200

Figure 6

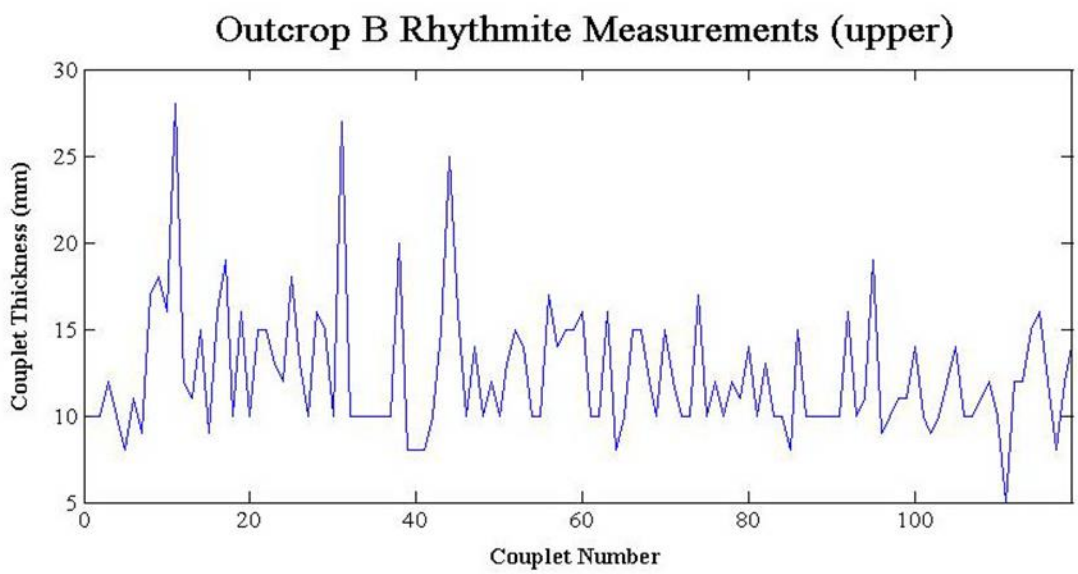
Outcrop B Rhythmite Measurements (upper)
Couplet Thickness (mm)
Couplet Number
5
10
15
20
25
30
0
20
40
60
80
100

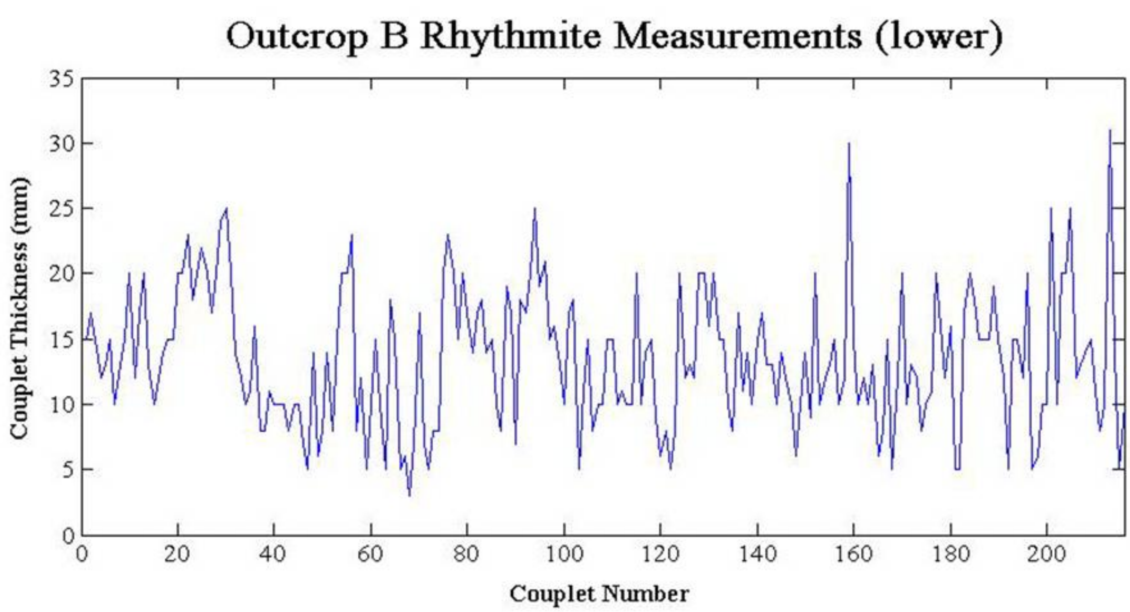
Outcrop B Rhythmite Measurements (lower)
Couplet Thickness (mm)
Couplet Number
0
5
10
15
20
25
30
35
0
20
40
60
80
100
120
140
160
180
200

Figure 7

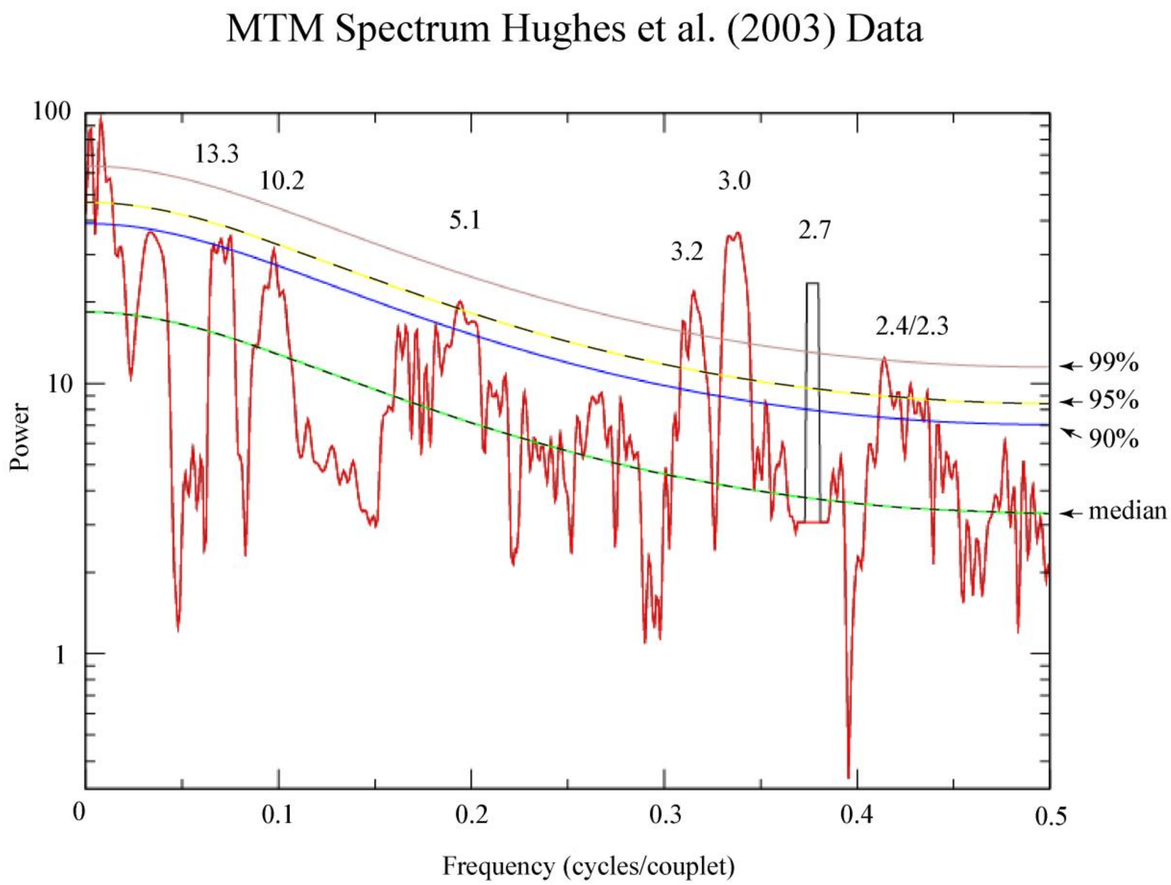
MTM Spectrum Hughes et al. (2003) Data
100
10
1
Power
0
0.1
0.2
0.3
0.4
0.5
Frequency (cycles/couplet)
13.3
10.2
5.1
3.2
3.0
2.7
2.4/2.3
99%
95%
90%
median

Figure 8

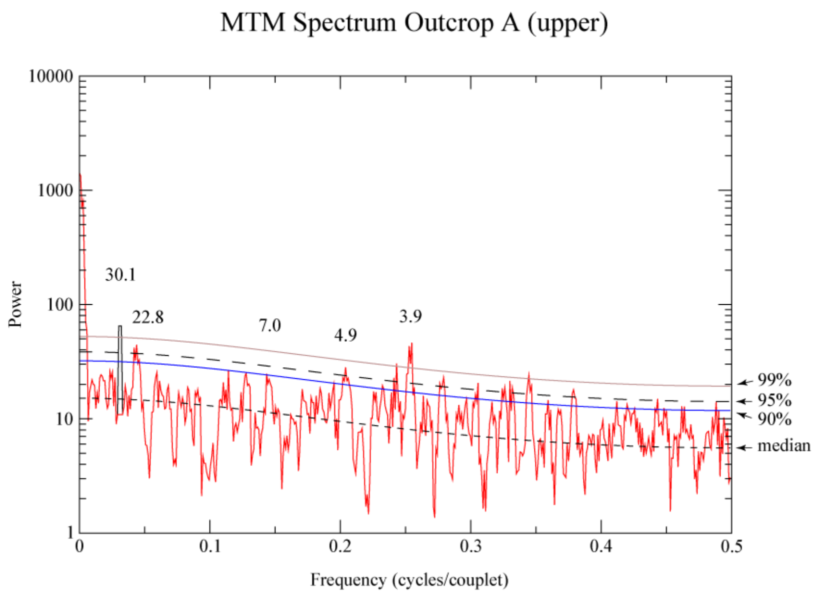
MTM Spectrum Outcrop A (upper)
Power
Frequency (cycles/couplet)
30.1
22.8
7.0
4.9
3.9
99%
95%
90%
median

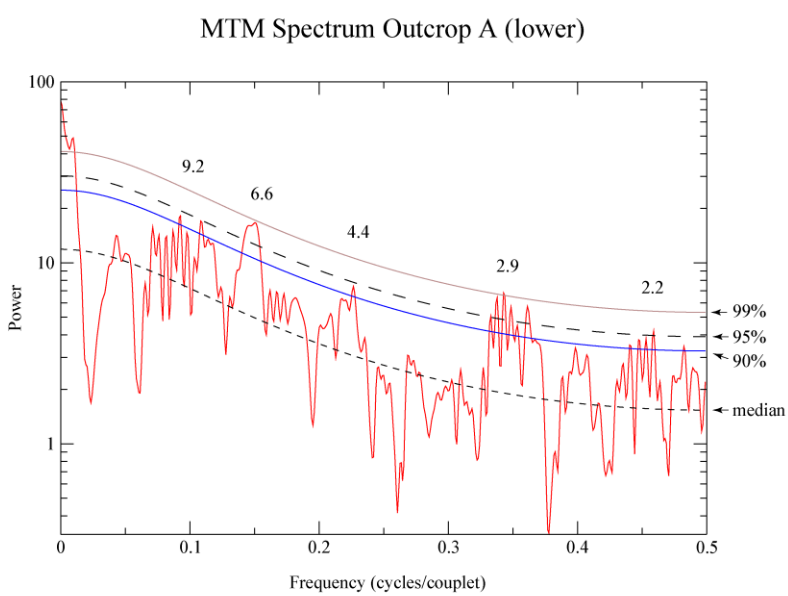
MTM Spectrum Outcrop A (lower)
Power
Frequency (cycles/couplet)
9.2
6.6
4.4
2.9
2.2
99%
95%
90%
median

Figure 9

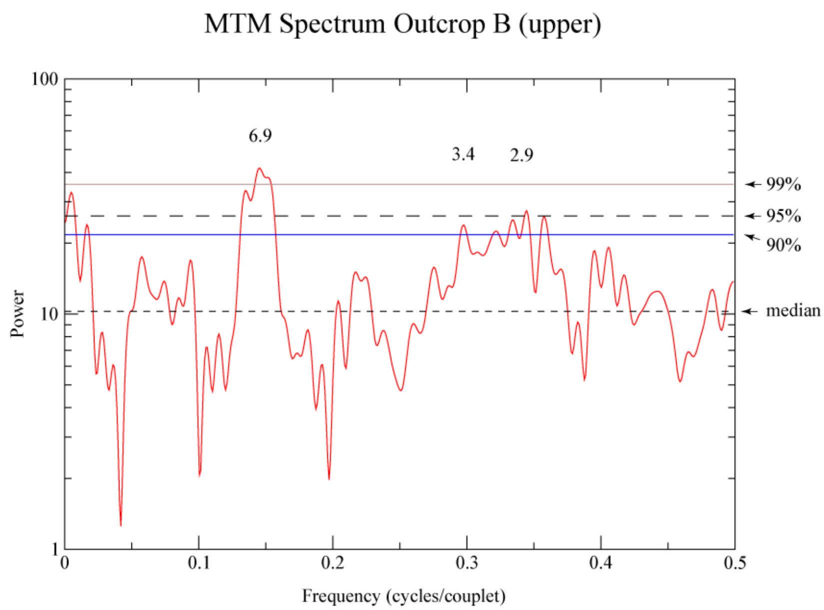
MTM Spectrum Outcrop B (upper)
6.9
3.4
2.9
99%
95%
90%
median
100
10
1
Power
0
0.1
0.2
0.3
0.4
0.5
Frequency (cycles/couplet)

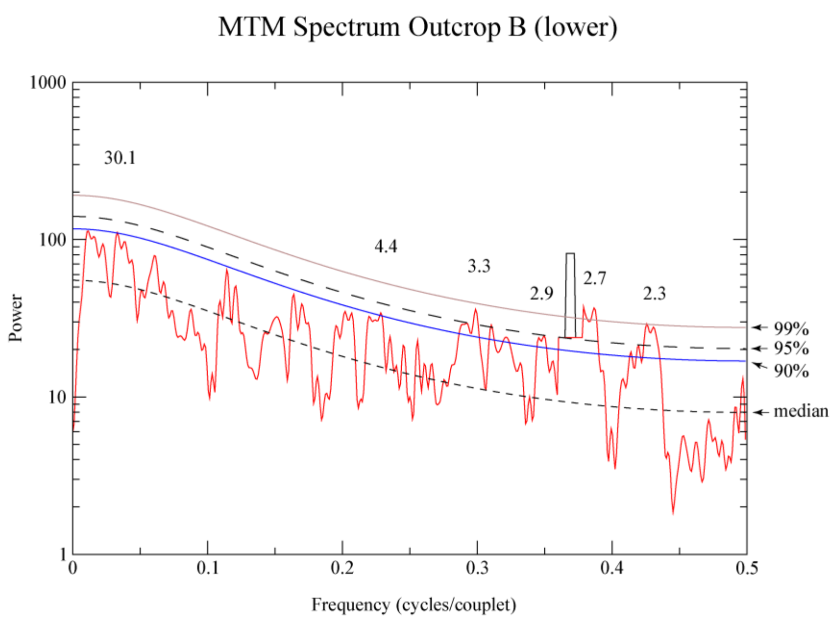
MTM Spectrum Outcrop B (lower)
30.1
4.4
3.3
2.9
2.7
2.3
99%
95%
90%
median
1000
100
10
1
Power
0
0.1
0.2
0.3
0.4
0.5
Frequency (cycles/couplet)